scientific reports

Check for updates

OPEN

Research on an intelligent fan cultural sustainability design method based on CPO-CNN-LSSVM

Kai Cheng[1,3]✉ & Nataliia Vladyslavivna Skliarenko[2,3]✉

The integration of intangible cultural heritage (ICH) into innovative products is a key focus in the intersection of culture and technology. This study addresses the core challenge of balancing cultural authenticity with functional requirements in smart home systems, using the household smart fan as a case study centered on Miao ethnic culture. To this end, we developed a hybrid methodology: the Fuzzy Analytic Hierarchy Process (FAHP) was first applied to quantify user emotional needs and Miao cultural style weights. Fuzzy Quality Function Deployment (FQFD) then translated these needs into critical design features. Finally, the Crested Porcupine Optimizer-Convolutional Neural Network-Least Squares Support Vector Machine (CPO-CNN-LSSVM) algorithm was employed to model the complex, nonlinear relationships and predict optimal design solutions. Our results demonstrate that this integrated approach effectively identifies culturally significant design features that align with user emotions, ensuring that products meet functional demands while embodying cultural value. The proposed framework offers a sustainable and systematic pathway for cultural inheritance through smart product innovation.

Keywords Emotional design, Intangible cultural heritage, Smart products, CPO, CNN, LSSVM

After rapid economic development and meeting material needs, consumer preferences have shifted. People now seek products that are emotionally resonant and rich in cultural and artistic depth. Meanwhile, China has enacted various policies to promote the inheritance and development of its traditional culture[1]. These policies aim to enhance both the nation's cultural soft power and international influence, as well as to strengthen cultural confidence and identity[2,3]. A key component of these initiatives is the preservation and transmission of distinctive ethnic cultures, such as that of the Miao people. Miao embroidery is an important economic source for Miao communities. It reflects the character and lifestyle of the Miao people, holding high artistic value and socio-cultural significance.

There is a growing interest among household consumers in modern innovative products that feature ethnic cultural elements. This has led to the emergence of culturally creative and innovative products. In 2023, China produced 1.54 billion cultural and creative products, with a market demand of 1.5 billion units. The total market value reached 88.05 billion yuan. Projections suggest output will grow to 1.73 billion units by 2030, showing substantial market potential for these products.

Technological advancements and better user experiences have drawn significant scholarly attention to smart home products. For example, Jiang[4] addressed smart home layout inefficiencies by proposing an optimized method using a real-number encoding genetic algorithm. Tang[5] examined the relationship between consumer value perception and smart home products from the perspective of platform ecosystem theory. Huang[6] investigated why elderly users avoid smart home products by creating a model linking product attributes, identity, trust, and avoidance. Tippe[7] analyzed how user behavior impacts life cycle assessment (LCA) using an interdisciplinary perspective. Tang[8] explored the effects of platform synergy on consumer value perception, using data from 405 smart home products on Amazon Japan.

In the realm of cultural products, the emergence of new technologies has also captured the interest of numerous scholars. For instance, Han[9] investigates the design of cultural and creative products and image

[1]Kyiv National University of Technologies and Design, Kyiv, Ukraine. [2]Lutsk National Technical University, Kyiv, Ukraine. [3]School of Design and Art, Shaanxi University of Science and Technology, Xi'an 710016, China. ✉email: ck389328336@gmail.com; nata_skliarenko@ukr.net

recognition based on Convolutional Neural Network (CNN) models. Cheng [10] examines whether the MPCM model can be simplified without compromising its predictive accuracy and explores the most suitable machine learning algorithms for creativity prediction. Liu [11] addresses the emotional demands of contemporary users and the promotion of culturally valuable Ming-style furniture by studying the Ming-style "warped table." It provides a systematic redesign process that encompasses analysis, Likert-weighted scoring, and Quality Function Deployment (QFD). This methodology enables quantitative analysis and parametric translation of traditional furniture imagery, significantly enhancing the product's cultural and emotional expression. Hu [12] Addressing limitations in current generative models—particularly in maintaining stylistic coherence and adapting to personalized preferences—introduces a novel image synthesis framework: the Evolutionary Adaptive Generative Aesthetic Network (EAGAN). This framework employs a synergistic mechanism based on integrated text-driven prompting, adaptive style modulation, and evolutionary optimization. Wang [13] explores the application of Zen aesthetics in contemporary furniture design within a sustainability context through rational data analysis, offering innovative insights and a reference framework for modern furniture design.

Although existing research has made significant progress in system construction, functional implementation, and cultural and user experience, it still generally overlooks users' emotional needs for traditional cultural elements. The focus of smart home product development is gradually shifting from a purely functional orientation to one that emphasizes cultural creativity and emotional resonance. Smart home products that incorporate ethnic minority cultural elements possess profound cultural heritage and unique styles, and can enhance the ethnic cultural atmosphere of home environments, strengthen emotional connections with consumers, and thereby drive market growth [14].

Traditional design approaches often fail to adequately capture the deep connections between users' emotional needs and cultural elements. Therefore, new methodologies are required to aid designers in understanding the emotional interaction mechanisms between users and products during the early stages of development, thereby facilitating the deep integration of Miao cultural elements into smart home products. Using the smart home fan as a case study, this research integrates machine learning algorithms with quantitative analysis methods to explore users' emotional needs for smart home products. The objective is to design smart home products that meet functional requirements while also responding to traditional cultural and emotional demands.

The main contributions of this research can be summarized as follows:

1. A three-layer mapping theoretical framework—demand-feature-cultural symbol—oriented toward culturally emotional design is proposed, addressing the gap in existing research regarding systematic modeling between cultural semantics and product design features.
2. Replacing traditional models like RF and BP (neural networks) with the CPO-CNN-LSSVM model establishes the mapping relationship between users' cultural emotional needs and design features, enhancing the accuracy of predicting emotional responses to home product design characteristics.
3. Through the design implementation of Miao culture in smart fans, this framework demonstrates its feasibility and effectiveness in achieving cultural heritage preservation and fostering emotional resonance with users.

The paper is organized as follows: Section II reviews relevant research methodologies. Section III presents the overall research framework, including the computation of the importance of Miao cultural elements and smart home design features. A mapping matrix is established between Miao cultural elements and smart home products to predict users' cultural and emotional needs. Finally, the design implementation and outcome analysis are presented. Section IV provides a discussion of the research methods, pathways, and design outcomes. Section V summarizes the research, identifies its limitations, and outlines directions for future work.

Related work

This study recruited volunteers aged 18 to 65 to conduct perceptual evaluations (in the form of ratings) of smart fan products. All methods were conducted in accordance with the relevant regulations of the Ethics Review Committee of Shaanxi University of Science and Technology. This research has been reviewed and approved by the Ethics and Morality Committee of Shaanxi University of Science and Technology, which consented to the user rating study on new energy vehicle interiors. Review number: IRBSUT20251089. All experimental participants completed the questionnaire survey with informed consent.

Kansei engineering

Kansei Engineering (KE) is defined as a product development methodology dedicated to translating users' emotions and perceptions (Kansei) into optimal product design parameters [15]. First proposed by Japanese scholars, KE was initially applied in the automotive industry and has since been expanded to numerous fields, including consumer electronics. The core objective of KE is to translate users' emotional needs into concrete product design elements, thereby enhancing user satisfaction and market competitiveness.

Recent years have witnessed a growing body of in-depth research within the field of KE. For instance, Li [16] proposed an opinion-mining method that integrates KE with machine learning to extract and quantify users' emotional responses from online reviews. In this study, five machine learning algorithms were compared, and the combination of a Support Vector Machine and Support Vector Regression (SVM-SVR) was demonstrated to achieve optimal performance. Yuan et al. [17] employed Support Vector Regression (SVR) to construct a mapping model between user-perceived needs and the core design features of nursing beds. Through weighted calculations, optimal design solutions were derived, leading to the identification of the best combination of design features for medical nursing beds. Wang et al. [18] proposed a hybrid SSA-LSTM-Attention model to enhance the emotional experience and customer satisfaction within new energy vehicle intelligent cockpits.

The implementation of KE generally follows a structured process: (1) Requirement Collection, where user emotional needs are gathered through surveys, interviews, and questionnaires; (2) Sentiment Analysis, which involves parsing user feedback to identify key affective factors; (3) Product Feature Definition, where emotional needs are translated into actionable design parameters and principles; (4) Design Development, during which the product is designed based on the prior analysis; and (5) User Testing and Evaluation, where prototypes are tested, feedback is collected, and iterative improvements are made.

Fuzzy analytic hierarchy process

The Fuzzy Analytic Hierarchy Process (FAHP) combines fuzzy mathematics with the Analytic Hierarchy Process (AHP) [19]. It aids in multi-objective decision-making, particularly when uncertainty and subjective judgments are prevalent [20,21].

By evaluating various user needs, FAHP assigns weights to them. This helps decision-makers spot the most important requirements. Its basic computational steps follow.

Step 1: Establish a hierarchical model. Define demand objectives and main influencing factors, then build a preliminary fuzzy hierarchy related to the demands.

Step 2: Build a fuzzy judgment matrix. For each upper-level element, compare the importance of its two subordinate elements. Convert fuzzy numbers to definite values, then establish the importance matrix using the 0.1–0.9 scale, as shown in Table 1.

Step 3: Given n comparison factors A^1, A^2, …, A_n, evaluate them using the 0.1–0.9 scale method shown in Table 1 to construct an importance evaluation matrix in the following format:

$$A = \begin{bmatrix} a_{11} & a_{12} & \cdots & a_{1n} \\ a_{21} & a22 & \cdots & a_{2n} \\ \vdots & \vdots & \ddots & \vdots \\ a_{n1} & a_{n2} & \cdots & a_{nn} \end{bmatrix} \tag{1}$$

Here, a_{ij} denotes the relative importance of indicator i compared to indicator j. The specific scaling rules are shown in Table 1. Matrix A must satisfy the conditions of a fuzzy complementary matrix: $0 < a_{ij} < 1$; $a_{ij} + a_{ji} = 1$; $a_{ii} = 0.5$; $(i, j = 1, 2, \ldots, n)$.

Step 4: Sum the rows of matrix A and compute the weights w_i:

$$a_i = \sum_{k=1}^{n} a_{ik}, (i, k = 1, 2 \cdots n) \tag{2}$$

$$\omega_i = \frac{1}{n} - \frac{1}{n-1} + \frac{2a_i}{n(n-1)} \tag{3}$$

Then, construct the single-layer exponential weight vector W.

$$W' = [\omega_1 \omega_2 \cdots \omega_n]^T \tag{4}$$

Based on this, construct the weight vector W for the single-layer indicators. Through the above steps, the weights for the criterion layer and the objective layer can be calculated separately, thereby determining the comprehensive weight of the objective layer to assist in identifying the core elements in decision-making.

Fuzzy quality function deployment

Fuzzy Quality Function Deployment (FQFD) is a way to develop products that combines a method for dealing with unclear information (fuzzy set theory) with Quality Function Deployment (QFD), which helps connect what customers want with the features of a product. QFD is a step-by-step tool that companies use to translate customer needs into product design ideas. FQFD enhances QFD by incorporating fuzzy set theory, making it more effective when dealing with complex or unclear information.

Scale	Implication
0.5	By comparison, the two elements are equally important
0.6	By comparison, one element is slightly more important than the other
0.7	By comparison, one element is obviously more important than the other
0.8	By comparison, one element is strongly more important than the other
0.9	By comparison, one element is extremely more important than the other
0.1, 0.2, 0.3, 0.4 (complementary)	If the element r_{ij} is obtained by comparing the element a_i with the element a_j,the element $r_{ji} = 1 - r_{ij}$ is obtained by comparing the element a_j withelement ai

Table 1. Criteria for comparing the importance of fuzzy hierarchical analysis method.

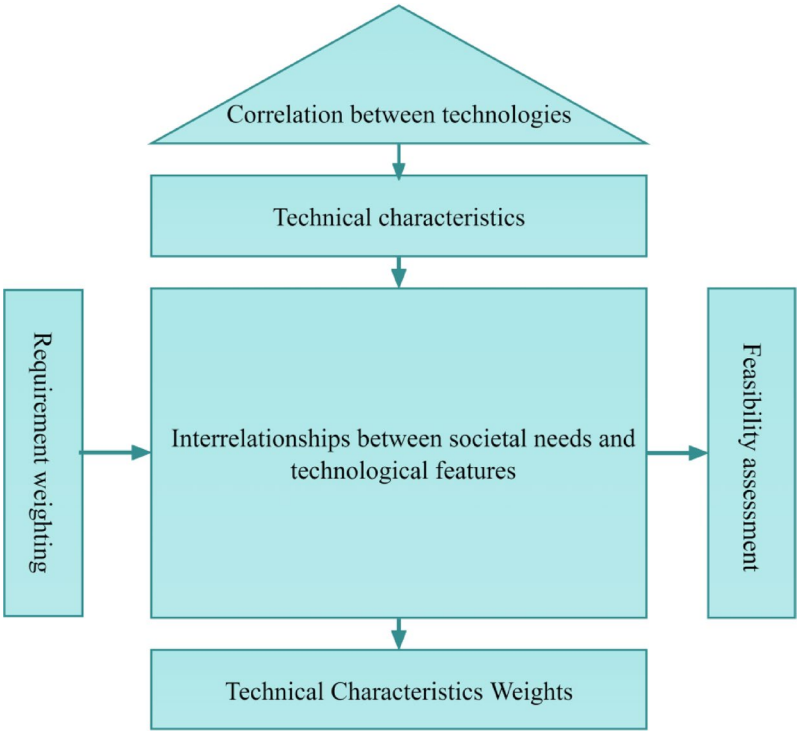

Fig. 1. Quality house construction.

Relevant symbol	Meaning expressed	Converted fuzzy number
None	No correlation	(0, 0, 0)
◁	Weak correlation	(1, 1, 3)
◯	Moderately weak correlation	(1, 3, 5)
◎	Moderate correlation	(3, 5, 7)
⊙	Moderately strong correlation	(5, 7, 9)
●	High correlation	(7, 9, 9)

Table 2. Correlation symbols and their corresponding triangular fuzzy numbers.

FQFD creates a clear way to connect what users want with the technical parts of a product. The primary tool FQFD utilizes is the House of Quality (HOQ) model. The HOQ helps show how different needs and technical features are linked. It accomplishes this using a chart, as illustrated in Fig. 1.

The FQFD process usually involves these steps:

1. Find out what customers want: Gather and organize customer needs through surveys, interviews, or other ways.
2. Define technical features: Review social, economic, and technical factors along with current product features. Identify the technical features and product details needed to meet customer needs.
3. Build Fuzzy Metrics: Use fuzzy processing on customer needs and technical details. Represent their connections with shapes like triangular fuzzy numbers. See Table 2 for fuzzy symbols.

Triangular fuzzy numbers are fuzzy sets defined by three parameters (typically denoted as a, b, c, where $a \le b \le c$). They integrate multi-variable influences through triangular membership functions, enhancing flexibility in describing uncertainty concepts. Parameters a and c represent the lower and upper bounds of the fuzzy number, respectively. Their difference (c-a) reflects the degree of fuzziness, where a larger value indicates higher uncertainty. Given two triangular fuzzy numbers $A = (a_1, b_1, c_1)$ and $B = (a_2, b_2, c_2)$, their basic operation rules are as follows:

$$A \oplus B = (a_1 + a_2, b_1 + b_2, c_1 + c_2)$$
$$A \otimes B = (a_1 \cdot a_2, b_1 \cdot b_2, c_1 \cdot c_2) \quad (5)$$
$$(A)^{-1} = \left(\frac{1}{a}, \frac{1}{b}, \frac{1}{c}\right)$$

4. Establish a Fuzzy Relationship Matrix: Construct a matrix to represent the fuzzy associations between customer requirements and technical characteristics, where matrix elements reflect the relative importance of different requirements and characteristics.
5. Fuzzy weight calculation: Based on the fuzzy relationship matrix, domain experts are invited to assign scores according to relevance symbols, thereby calculating the weights of each technical characteristic relative to customer requirements. The formulas for absolute weight QR_j and relative weight Q_j are as follows:

$$QR_j = \sum_{i=1}^{n} W_i R_{ij} \quad (j = 1, 2, 3 \ldots n) \quad (6)$$
$$Q_j = \frac{QR_j}{\sum_{i=1}^{n} QR_j}$$

Among these, W_i denotes the comprehensive weighting of user requirements, while R_{ij} represents the relationship assignment between requirements and characteristics.

6. Defuzzification: Defuzzify fuzzy weights to convert them into deterministic values for design decision support. The centroid method is commonly used. For a fuzzy number $QR_j = (a,b,c)$, its defuzzification formula is:

$$QR\mathrm{j} = \frac{a + b + c}{3} \quad (7)$$

Through the above steps, FQFD can objectively identify key product design features by accurately capturing users' subjective needs, thereby providing a theoretical basis for subsequent development.

CPO-CNN-LSSVM model

A hybrid learning framework can be constructed by integrating Convolutional Neural Networks (CNN) and Least Squares Support Vector Machines (LSSVM) through model fusion. This integration leverages the complementary strengths of CNNs in spatial feature extraction and LSSVMs in managing complex regressions.

The Crested Porcupine Optimizer (CPO) is a metaheuristic algorithm recognized for its robust performance on multimodal and high-dimensional optimization problems, as well as its rapid convergence and global search capability [22]. The CPO algorithm is modeled after four defensive behaviors exhibited by crested porcupines when threatened: visual deterrence, vocal warning, scent release, and physical attack, which are hierarchically engaged based on the perceived threat level [23].

The algorithm's search space is conceptualized as four distinct defense zones, as visualized in Fig. 2. In Zone A, corresponding to the crested porcupine being farthest from a threat, the first strategy (visual deterrence) is applied. As the search process intensifies (Zones B and C), the subsequent strategies are activated. Zone D represents the final stage, where the direct attack strategy is employed if all others prove ineffective.

Let the objective function be denoted as $f(x)$, where x represents the vector of variables to be optimized. The update rule for the position of individuals in the CPO algorithm can be expressed as:

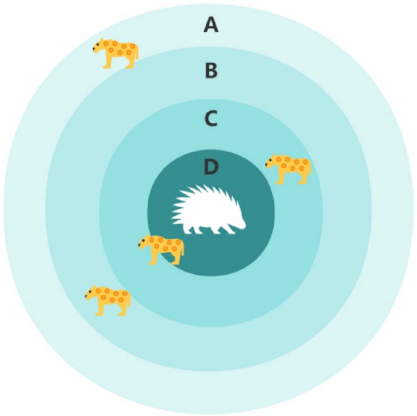

Fig. 2. Crown porcupine defense area.

$$x_{t+1} = x_t + \sum_{i=1}^{N} \Delta x_i \tag{8}$$

Here, x_{t+1} represents the solution vector of the next generation, x_t denotes the solution vector of the current generation, N indicates the population size, and Δx_i is the adjustment amount for the solution vector of the i-th pig.

Step 1: Initialization Phase.

Within the search space, randomly initialize the positions of each individual in the population according to formula (9):

$$x_i = L + r \times (U - L) \quad i = 1, 2, \ldots nN' \tag{9}$$

Here, N' represents the number of individuals, X_i denotes the i-th candidate solution, L and U are the lower and upper bounds of the search range, respectively, and r is a random vector within the range [0,1]. The initial population can be expressed as follows:

$$X = \begin{bmatrix} X_1 \\ X_2 \\ \vdots \\ X_i \\ \vdots \\ X_N \end{bmatrix} = \begin{bmatrix} x_{1,1} & x_{1,2} & \cdots & x_{1,j} & \cdots & x_{1,d} \\ x_{2,1} & x_{2,1} & \cdots & x_{2,j} & \cdots & x_{1,d} \\ \vdots & \vdots & \vdots & \vdots & \vdots & \vdots \\ x_{i,1} & x_{i,2} & \cdots & x_{i,j} & \cdots & x_{i,d} \\ \vdots & \vdots & \vdots & \vdots & \vdots & \vdots \\ x_{N,1} & x_{N,2} & \cdots & x_{N,j} & \cdots & x_{N,d} \end{bmatrix} \tag{10}$$

Here, d denotes the dimension of the given problem.

Step 2: Cyclic Population Reduction Technique.

This strategy accelerates convergence by dynamically adjusting population size during optimization: periodically removing some individuals to reduce computational overhead, then reintroducing them later to enhance diversity and prevent getting stuck in local optima [24]. The number of cycles is controlled by variable T, with the specific formula as follows:

$$N = N_{\min} + \left(N' - N_{\min}\right) \times \{1 - \left\{\frac{t\%\frac{T_{\max}}{T}}{\frac{T_{\max}}{T}}\right\}\} \tag{11}$$

where T is the variable determining the number of iterations, t is the current function evaluation, T_{max} is the maximum number of function evaluations, % denotes the remainder or modulo operator, and N_{min} is the minimum number of individuals in the newly generated population, ensuring the population size does not fall below N_{min}.

Step 3: Exploration Phase.

Corresponding to the medium-to-long-range defensive behavior of the crowned porcupine, this phase involves two strategies:

Defense Strategy: Simulates changes in distance between the predator and the crowned porcupine:

- If the predator approaches, intensify localized search;
- If the predator retreats, expand the exploration range.

Mathematically expressed as:

$$x_i^{t+1} = x_i^t + \tau_1 \times \left|2 \times \tau_2 \times x_{CP}^t - y_i^t\right| \tag{12}$$

x_{CP}^t represents the optimal solution obtained at iteration t through function evaluation. y_i^t denotes the vector generated between the current CP and a randomly selected CP from the population, representing the predator's position at iteration t. τ_2 is a random number based on a normal distribution. τ_2 is a random value within the interval [0, 1].

Defense Strategy: The CP mimics threatening sounds to deter predators:

$$x_i^{t+1} = (1 - U_1) \times x_i^t + U_1 \times \left(y + \tau_3 \times x\left(_{r1}^{t} - x_{r2}^t\right)\right) \tag{13}$$

Among them, r_1 and r_2 are two random integers between [1, N], generated as random values between 0 and 1.

Step 4: Developmental Stage: Defensive behaviors within short distances also encompass two strategies:

Defense Strategy: In this strategy, CP secretes a foul odor to deter predators from approaching. Mathematically simulated as follows:

$$x_i^{t+1} = (1 - U_1) \times x_i^t + U_1 \times \left(x_{r_1}^t + S_i^t \times \left(x_{r_2}^t - x_{r3}^t\right) - \tau_3 \times \delta \times \gamma_t \times S_i^t\right) \tag{14}$$

r_3 is a random number between [1, N], δ is a parameter controlling the search direction, x_i^t is the position of the *i*-th individual at iteration t, γ_t is the defense factor defined by the equation. τ_3 is a random value within the interval [0, 1] and represents the odor diffusion factor.

Defense Strategy: When a predator approaches very close to the CP, it attacks using its short, thick feathers. Mathematically simulated as follows:

$$x_i^{t+1} = x_{CP}^t + (\alpha\,(1-\tau_4) + \tau_4) \times \left(\delta \times x_{CP}^t - x_i^t\right) - \tau_5 \times \delta \times \gamma_t \times F_i^t \tag{15}$$

x_{CP}^t represents the optimal solution obtained, α denotes the convergence speed factor, τ_4 is a random value within the interval [0,1], and F_i^t is the average force affecting the CP of the i-th predator.

Initially developed for image processing, Convolutional Neural Networks (CNNs) are now being applied extensively to time series forecasting tasks [25]. CNNs capitalize on local perception and weight-sharing mechanisms. These models are effective at capturing local dependencies and latent patterns in time series data. A typical CNN architecture, as shown in Fig. 2, includes an input layer, convolutional layers, pooling layers, fully connected layers, and an output layer.

The input layer receives time series data, usually structured in two dimensions (time steps × features). The convolutional layer uses one-dimensional convolution operations to extract local features. The kernel size defines the temporal receptive field. The pooling layer then downsamples the feature sequence. This process reduces dimensionality while retaining key feature information. Feature maps from the convolutional and pooling layers are flattened into one-dimensional vectors. These are fed into fully connected layers to abstract and integrate high-level features. The output layer generates final predictions, whether for regression or classification tasks.

Convolution layers form the foundation of CNNs, consisting of a series of convolutional kernels. Each filter slides across the input image to perform a convolution operation. This operation extracts features by applying the convolutional kernel to the input data. The calculation formula is as follows:

$$H_i = g\,(W_i \otimes X_{i-1} + b_i) \tag{16}$$

In the formula: H_i denotes the feature quantity of the *i*-th layer output, X_{i-1} represents the input data, W_i and b_i denote the bias and weights, $\otimes$ denotes the convolution operation, and g denotes the ReLU activation function.

Pooling layers typically follow convolutional layers. Their function is to downsample feature maps, reducing the number of parameters and computational load while imparting translation invariance to the features. The calculation formula is as follows:

$$H_{i+1} = P\,(H_i) \tag{17}$$

Among these, P represents the pooling function, while H_i and H_{i+1} denote the feature quantities before and after pooling.

The Least Squares Support Vector Machine (LSSVM) is a variant of the standard Support Vector Machine (SVM). It uses a least squares linear system as its loss function. This approach replaces standard SVMs' inequality constraints with equality constraints. As a result, LSSVM offers reduced computational complexity, faster convergence, and improved regression accuracy for nonlinear predictions [26,28]. The regression function for the LSSVM model is defined by Eq. (18).

$$f\,(x) = \omega \times \phi\,(x) + b \tag{18}$$

In the corresponding equation, the parameters are defined as follows: ω is the weight vector, $\varphi(x)$ is the feature mapping function, and b is the bias term. Guided by the principle of structural risk minimization, the LSSVM optimization problem can be formulated as follows:

$$\begin{cases} \min J\,(\omega, b, e) = \dfrac{1}{2}\left\|\omega^2\right\| + \dfrac{1}{2} r \displaystyle\sum_{i=1}^{n} e_i^2 \\ s.t. y_i = \omega^T \phi\,(x_i) + b + e_i \end{cases} \tag{19}$$

In the equation: e_i represents the fitting error; y denotes the penalty factor.

Introducing the Lagrange multiplier λ_i and differentiating the above equation to eliminate ω and e yields the LSSVM prediction model:

$$f\,(x) = \sum_{i=1}^{N} \lambda_i K\,(x_i, x_j) + b \tag{20}$$

In the formula: $K(x_i, x_j)$ is the kernel function, representing the nonlinear mapping from the input space to the high-dimensional feature space. This paper employs the Gaussian kernel function.

In traditional machine learning, a model's predictive performance is heavily influenced by the configuration of its hyperparameters. Conventional methods—including empirical tuning and grid search—are prone to overfitting, underfitting, or getting stuck in local optima, thereby limiting the model's generalization capability. To address these issues, the Crown Porcupine Optimizer (CPO) algorithm is introduced for automatic

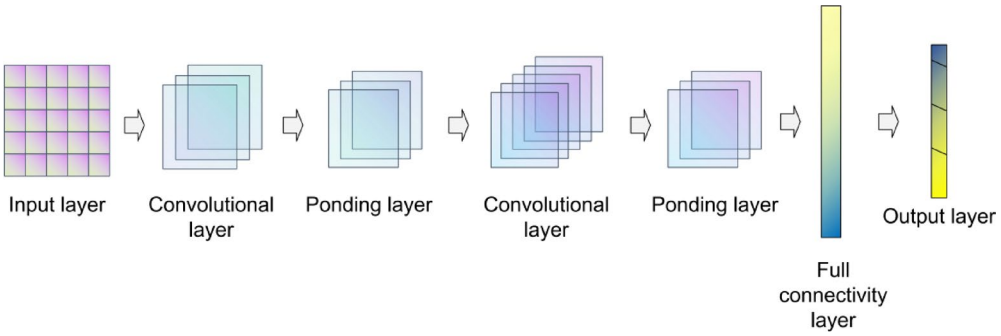

Fig. 3. CNN basic structure.

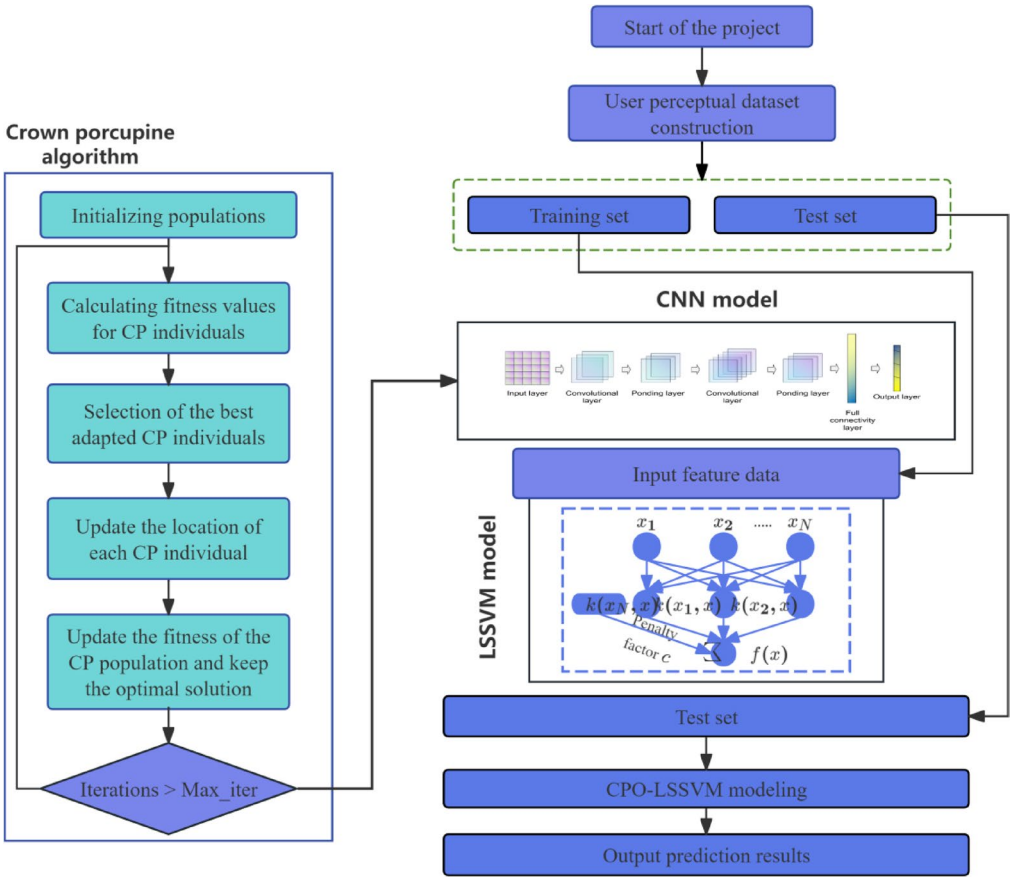

Fig. 4. Model building process.

hyperparameter optimization of the CNN-LSSVM model, aiming to enhance its predictive accuracy and robustness. Within this hybrid architecture, the CNN primarily handles feature extraction. The CPO-optimized CNN functions as a powerful feature extractor, mapping raw data into a high-dimensional, linearly separable feature space. At the same time, the LSSVM performs efficient regression within this feature space (Fig. 3).

The specific steps for CPO-optimizing the CNN-LSSVM model are illustrated in Fig. 4. First, CPO algorithm parameters are set, including population size, maximum iterations, optimization dimensions, parameter bounds, and other relevant hyperparameters. Next, population positions are randomly initialized, with CNN hidden layer node count, learning rate, and LSSVM regularization parameter serving as optimization variables. Next, evaluate the fitness of each individual in the population using the mean squared error of the CNN-LSSVM model on the validation set as the fitness function. Subsequently, rank the current population individuals based on their fitness values, select the optimal individual in the current iteration, and compare it with the historical global optimum. If superior, update the global optimum parameters. Next, the termination condition (e.g., reaching the maximum iteration count) is checked. If not met, the population positions are updated and optimization continues; otherwise, the iteration ends. Finally, the optimal hyperparameter configuration obtained through

CPO optimization is applied to the CNN-LSSVM model to predict user sentiment and interaction perception, outputting the final results.

Research framework

This study proposes a systematic hybrid framework to facilitate the integration of traditional cultural elements with the emotional design characteristics of modern products, thereby supporting the design and validation of smart home products that incorporate traditional imagery. The overall research framework is illustrated in Fig. 5 and comprises the following steps:

First, data were collected using web crawling technology. This included 12,571 online user reviews of smart home products from Amazon and 100 product images of a representative category (smart fans). Concurrently, 50 traditional Miao ethnic patterns were acquired through questionnaire surveys (with 200 participants) and from cultural heritage databases, including the National Museum of Ethnicities. Latent Dirichlet Allocation (LDA) topic modeling was then applied to the product reviews to extract high-frequency emotional vocabulary. The number of topics ($k = 5$) was determined by perplexity evaluation. A panel of five ethnology experts annotated the emotional vocabulary for the traditional patterns through focus group discussions. A dual-dimensional (product–culture) emotional vocabulary database was subsequently constructed.

Second, the FAHP was used to calculate the weights of the sentiment lexicon categories from both dimensions. This process enabled the selection of core sentiment sets (with a weight threshold greater than 0.1) for both smart home products and traditional Miao patterns, thereby reducing potential researcher bias. Furthermore, a semantic deconstruction of the core product affective terms was performed to extract their implicit design characteristics. The FQFD method was then employed to construct a House of Quality (HOQ) matrix, which mapped user needs to design characteristics, thereby identifying the key product design features.

To predict the correlations between product affective vocabulary and design characteristics, a mapping matrix was established based on expert affective ratings, serving as the training dataset. Simultaneously, a second mapping matrix was established, linking product design features to Miao pattern vocabulary through evaluations by a panel of eight cultural semiotics experts. This matrix served as the core dataset for analyzing cultural-design associations. The optimized CPO-CNN-LSSVM model was then employed to calculate the emotional association strengths between smart home product features and Miao cultural styles, which identified the optimal design and cultural style combinations.

Finally, based on the model's predictions, the optimal design and style features were selected for implementation, resulting in smart home product designs that harmonize traditional cultural imagery with modern functional requirements. For model evaluation, the performance of the proposed CPO-CNN-LSSVM model was compared with that of seven benchmark models (including SVM, LSTM, and ResNet-50) on a unified test set. Additionally, Shapley Additive exPlanations (SHAP) were employed to interpret the model and identify the most influential design features.

Research process

Acquisition of emotional vocabulary for smart home fans

Extraction of emotional vocabulary for smart home fans

Traditional manual data collection methods for acquiring product images and user reviews are subject to several limitations: low efficiency due to manual browsing and saving, limited coverage often restricted to static content from a few platforms, inability to capture dynamic content (e.g., JavaScript-loaded pagination) reliably, poor data consistency from manual organization, and insufficient timeliness for tracking new products or sentiment shifts.

In contrast, web crawling technology effectively addresses these limitations through automation. It facilitates continuous data scraping from diverse sources, including e-commerce platforms (e.g., Amazon, Taobao), social media, and specialized forums. This approach enables precise extraction of image links and user evaluations.

In this study, we employed web crawling to collect 12,571 raw reviews and associated product images using keywords such as "smart home products" and "home fans." A rigorous data cleaning pipeline was then implemented to ensure data quality. This included: (1) removing duplicate entries and advertisements; (2) filtering out non-textual content and robot-generated reviews; and (3) standardizing linguistic expressions, including correcting spelling errors and translating non-English comments into English.

From the cleaned corpus, high-frequency vocabulary was statistically analyzed, and descriptive adjectives were systematically extracted as candidate emotional descriptors. A panel of three domain experts conducted a rigorous manual validation process to finalize the emotional lexicon. The validation was based on the pre-defined criteria detailed in Table 3, which were calibrated using the actual high-frequency terms obtained from the analysis. These criteria included contextual relevance, emotional polarity, and emotional intensity. Any term with low contextual relevance or exhibiting disagreement among experts was discarded. The final consolidated emotional lexicon served as a reliable foundation for analyzing user emotional needs.

This methodology, grounded in empirically derived high-frequency terms, provides end-to-end support from initial market insight to technical validation, facilitating a transition from experience-driven to data-driven design decisions.

Following data collection, image samples were selected based on visual similarity and high clarity. A subset comprising four-fifths of the qualified images was selected as the test set. During this process, images with inconsistent perspectives were eliminated, and all image dimensions were standardized. A sample of 100 household smart fan appearances is displayed and analyzed on a single plane in Fig. 6.

Concurrently, sentiment-descriptive texts for smart home fans, obtained via web crawling, were integrated and analyzed using a Latent Dirichlet Allocation (LDA) topic model to identify key sentiment descriptors [29,31]. This analysis identified 10 distinct topics, as shown in Fig. 7. The corresponding topic visualization, presented

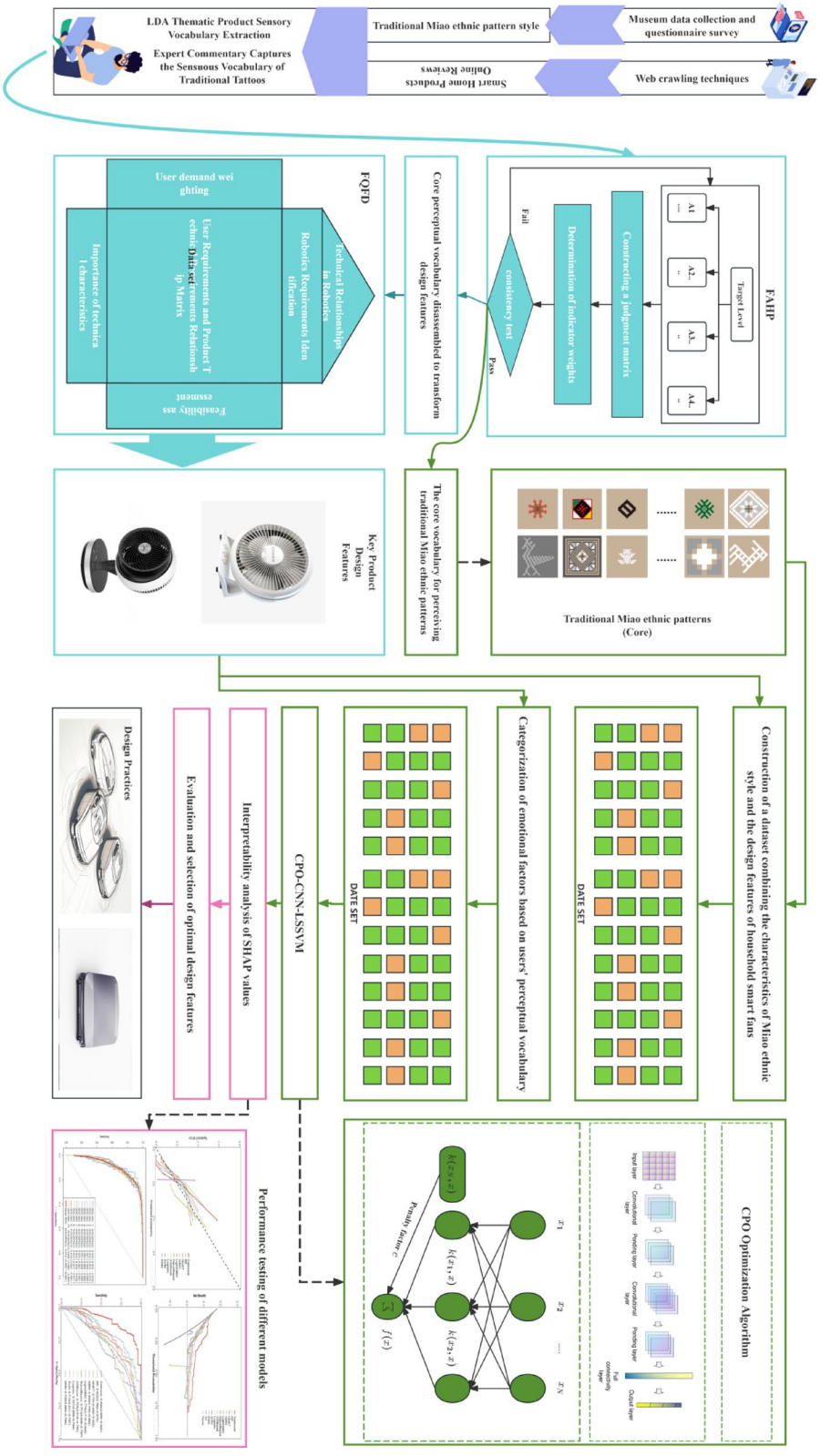

Fig. 5. Systematic mixed modeling research framework.

Criterion	Category	Description	Representative Examples from High-Frequency Vocabulary
Contextual Relevance	High	The word is directly and strongly related to the usage scenario and user experience of smart home fans	"User-friendly", "Powerful", "Quiet"
	Medium	The word is indirectly related to the product or user experience, or is relevant only in specific contexts	"Compact", "Unique", "Simple"
	Low	The word is unrelated to the product or user experience	"Delicious", "Political" (Discarded)
Emotional Polarity	Positive	Expresses satisfaction, preference, or praise	"Intelligent", "Reliable", "Convenient"
	Neutral	States a fact without clear emotional inclination	"Compact", "White"
	Negative	Expresses dissatisfaction, criticism, or disappointment	"Noisy", "Fragile"
Emotional Intensity	Strong	Conveys an extreme or very strong emotion	"Extremely Reliable", "Very Powerful"
	Medium	Conveys a clear but moderate emotion	"Comfortable", "Durable"
	Weak	Conveys a slight or uncertain emotion	"Okay", "Fine" (Discarded)

Table 3. Criteria for manual validation and categorization of emotional words. The final categorization of each emotional word required consensus from at least two experts. In cases of disagreement, a third expert was consulted to make a final arbitration. Examples in this table are drawn from the actual high-frequency vocabulary obtained through statistical analysis.

Fig. 6. Perceptual pictures of domestic household smart fans.

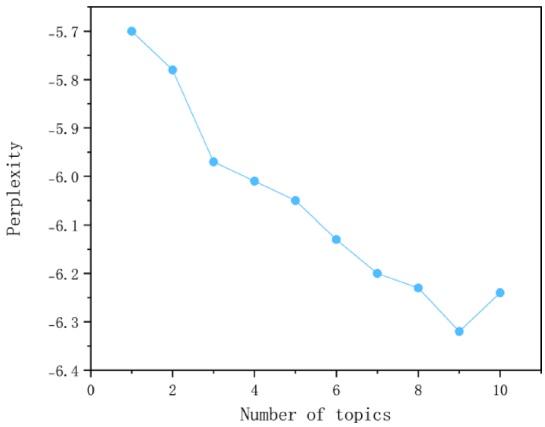

Fig. 7. Theme word perplexity.

in Fig. 8, clearly displays the affective vocabulary associated with each theme along with their respective weight distributions.

From this analysis, 70 affective engineering-related descriptors were extracted (Fig. 9), forming the foundation for a standardized affective lexicon. Subsequently, the top 15 affective terms by weight were selected through expert panel discussions; their specific distribution is provided in Table 4.

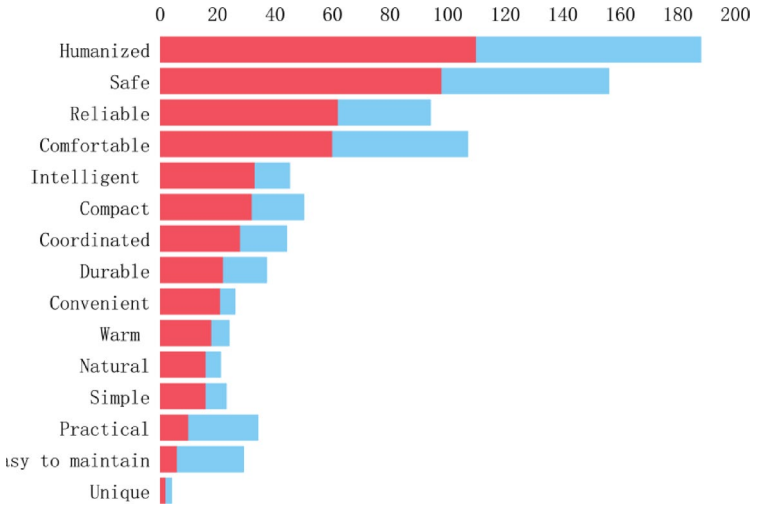

Fig. 8. LDA theme visualization results.

Fig. 9. Relevant Perceptual Engineering Descriptors.

User-friendly	Reliable	Compact
Safe	Comfortable	Well-balanced
Intelligent	Convenient	Durable
Warm	Natural	Simple
Practical	Easy to maintain	Unique

Table 4. The 15 most frequent emotional vocabulary words.

Core sentimental vocabulary acquisition based on FAHP

The sheer diversity of emotional vocabulary associated with smart home fans can complicate the evaluation process for researchers. Therefore, to streamline the evaluation, a fuzzy hierarchical model was constructed based on the previously analyzed 15 emotional vocabulary terms, and the core emotional vocabulary was calculated. This approach effectively simplifies the evaluation of factors related to smart home fans.

The criterion layer of the model consists of four primary indicators: emotional needs, functional needs, sensory needs, and operational needs. At the solution layer, the emotional needs indicator is defined by "sense of security," "warmth," "user-friendliness," and "comfort." The overall structure of this hierarchical model for smart home fan emotional vocabulary is depicted in Fig. 10.

Based on the affective vocabulary hierarchical model for smart home fans (Fig. 8), 15 experts in relevant fields were invited to rate the importance of each influencing factor. A judgment matrix was constructed through pairwise comparisons of the impact of each factor on the system objectives. Following the computational procedures defined in Eqs. (1) and (2), the weight values for each smart home fan requirement were calculated sequentially, and fuzzy consistency checks were performed concurrently. Subsequently, a fuzzy judgment matrix for the criterion layer was established. The results of the expert scoring and weight calculations are presented below.

$$A = \begin{bmatrix} & B1 & B2 & B3 & B4 \\ B1 & 0.5 & 0.7 & 0.4 & 0.6 \\ B2 & 0.3 & 0.5 & 0.3 & 0.6 \\ B3 & 0.6 & 0.7 & 0.5 & 0.7 \\ B4 & 0.4 & 0.4 & 0.3 & 0.5 \end{bmatrix}, w = \begin{matrix} B1 \\ B2 \\ B3 \\ B4 \end{matrix} \begin{bmatrix} 0.2833 \\ 0.2 \\ 0.3333 \\ 0.1833 \end{bmatrix}$$

Construct a fuzzy judgment matrix for each sub-criterion level, and derive the matrix score and weight calculation results for *B*1 as follows:

$$B_1 = \begin{matrix} \\ C1 \\ C2 \\ C3 \\ C4 \\ C5 \end{matrix} \begin{matrix} C1 & C2 & C3 & C4 & C5 \\ 0.5 & 0.4 & 0.4 & 0.4 & 0.6 \\ 0.6 & 0.5 & 0.6 & 0.7 & 0.7 \\ 0.6 & 0.4 & 0.5 & 0.6 & 0.7 \\ 0.6 & 0.3 & 0.4 & 0.5 & 0.7 \\ 0.4 & 0.3 & 0.3 & 0.3 & 0.5 \end{matrix}, w = \begin{matrix} C1 \\ C2 \\ C3 \\ C4 \\ C5 \end{matrix} \begin{bmatrix} 0.18 \\ 0.26 \\ 0.23 \\ 0.2 \\ 0.13 \end{bmatrix}$$

Construct a fuzzy judgment matrix for each sub-criterion level, and derive the matrix score and weight calculation results for *B*2 as follows:

$$B_2 = \begin{matrix} \\ C6 \\ C7 \\ C8 \end{matrix} \begin{matrix} C6 & C7 & C8 \\ 0.5 & 0.6 & 0.7 \\ 0.6 & 0.5 & 0.6 \\ 0.3 & 0.6 & 0.5 \end{matrix}, w = \begin{matrix} C6 \\ C7 \\ C8 \end{matrix} \begin{bmatrix} 0.4333 \\ 0.2667 \\ 0.3 \end{bmatrix}$$

Construct a fuzzy judgment matrix for each sub-criterion level, and derive the matrix score and weight calculation results for *B*3 as follows:

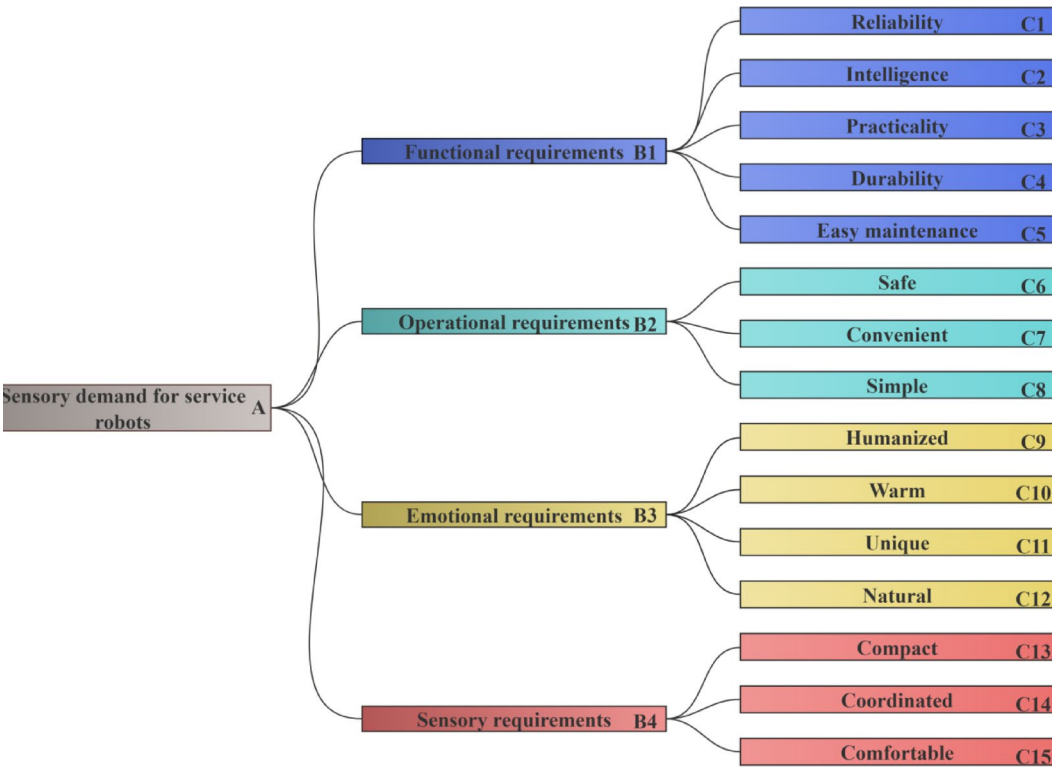

Fig. 10. Hierarchical model of perception vocabulary for household smart fans.

$$B_3 = \begin{array}{c} \\ C9 \\ C10 \\ C11 \\ C12 \end{array} \begin{array}{c} \begin{array}{cccc} C9 & C10 & C11 & C12 \end{array} \\ \begin{bmatrix} 0.5 & 0.4 & 0.6 & 0.6 \\ 0.6 & 0.5 & 0.6 & 0.7 \\ 0.4 & 0.4 & 0.5 & 0.6 \\ 0.4 & 0.3 & 0.4 & 0.5 \end{bmatrix} \end{array} \quad w = \begin{array}{c} \\ C9 \\ C10 \\ C11 \\ C12 \end{array} \begin{bmatrix} 0.2667 \\ 0.3167 \\ 0.2333 \\ 0.1833 \end{bmatrix}$$

Construct a fuzzy judgment matrix for each sub-criterion level, and derive the matrix score and weight calculation results for *B*4 as follows:

$$B_4 = \begin{array}{c} \\ C13 \\ C14 \\ C15 \end{array} \begin{array}{c} \begin{array}{ccc} C13 & C14 & C15 \end{array} \\ \begin{bmatrix} 0.5 & 0.4 & 0.4 \\ 0.6 & 0.5 & 0.4 \\ 0.6 & 0.6 & 0.5 \end{bmatrix} \end{array} \quad w = \begin{array}{c} \\ C13 \\ C14 \\ C15 \end{array} \begin{bmatrix} 0.2667 \\ 0.3333 \\ 0.4 \end{bmatrix}$$

The consistency ratio (*CR*) values for factors *A*, *B*1, *B*2, *B*3, and *B*4 were calculated as 0.0313, 0.032, 0.0444, 0.0188, and 0.0222, respectively. All values are below the 0.1 threshold, confirming that the judgment matrices passed the consistency test. The composite weight values for the factors were obtained by multiplying the first-level weight values by the corresponding second-level weight values. These composite weights were then ranked; the results are presented in Table 5.

The weighting of emotional factors for smart home fans helps designers prioritize directions that align with consumer needs, thereby improving overall design efficiency. In this study, nine key emotional factors with weights exceeding 0.6 were selected and applied to the design of smart home fans. Subsequently, these factors were clustered into conceptual dimensions to facilitate the construction of an evaluation matrix that links emotional needs to smart fan design characteristics.

Specifically, “Intelligence” reflects technological sophistication, “Practicality” denotes effective functional implementation, and “Safety” constitutes the foundational element for user trust. These three elements collectively form the “Intelligent Stability” dimension, which conveys technological credibility and ensures stable, reliable functionality. This dimension establishes a design principle centered on intelligent reliability.

"Humanization," "warmth," "comfort," and “harmony” represent a progressive emotional experience: humanization pertains to adaptive interaction, warmth cultivates an emotional ambiance, comfort addresses physiological sensations, and Harmony emphasizes overall consistency. Together, they constitute the “Emotional Comfort” dimension, which reflects a comprehensive response to users’ psychological and physiological needs, conveying emotional warmth in human–machine interaction.

At the cultural expression level, “Uniqueness” and “Harmony” are complementary: Uniqueness emphasizes the distinctiveness of Miao cultural elements, while Harmony focuses on their integration with modern product forms. Together, they define the “Harmonious Charm” dimension, which preserves the traditional cultural spirit while achieving a harmonious unity within contemporary home contexts.

In summary, the nine affective terms are integrated into three core design dimensions: "Intelligent Stability," "Emotional Comfort," and "Harmonious Charm." This framework provides a theoretical foundation and practical guidance for the emotional design of smart home fans.

Acquisition of sensory vocabulary characterizing miao style features

Sensory vocabulary acquisition

The precise identification of unique stylistic characteristics is crucial for advancing intelligent technology-driven innovation in the design of traditional Miao patterns. This study adopted an integrated methodology combining the FAHP with questionnaire surveys, implemented in the following steps:

First, a systematic selection of representative pattern samples from traditional Miao motifs was conducted through expert interviews, establishing them as the core subjects of this research. Concurrently, experts from relevant fields—including graphic, product, service, and fashion design—were invited to participate in systematic discussions to define the stylistic characteristics of traditional Miao patterns.

Second, based on the interview findings, feature terms related to the stylistic characteristics of Miao patterns were organized, refined, and consolidated into a definitive set of stylistic descriptors, which are presented in Table 6.

Acquisition of core emotional vocabulary based on FAHP

Building on the identified stylistic characteristics and representative patterns, a questionnaire was developed and distributed to embroiderers and domain experts utilizing systematic surveys and in-depth interviews. The surveys and interviews focused on three core aspects: the stylistic characteristics of Miao traditional embroidery patterns, their intrinsic connection to the profound ethnic culture, and key considerations for the modernization of traditional embroidery.

Following exhaustive data collection and rigorous inductive analysis, a fuzzy hierarchical model was constructed that accurately captures the stylistic features of Miao traditional patterns. This model, illustrated in Fig. 11, provides a theoretical framework for in-depth research.

	Reliability C1	Intelligent C2	Practical C3	Durable C4	Easy to Maintain C5	Safe C6	Convenient C7	Simple C8
Weight	0.051	0.0737	0.0652	0.0567	0.0368	0.0867	0.0533	0.06
	Humanized C9	Warm C10	Unique C11	Natural C12	Small C13	Coordinated C14	Comfortable C15	–
Weight	0.0889	0.1056	0.0778	0.0611	0.0489	0.0611	0.0733	–

Table 5. Combined weight values of perceptual factors for household smart fans.

Complexity	Pictographic representation	Harmonious arrangement	Hierarchy
			
Irregular	Rich	Narrative	Compositionally Complete
			
Continuous	Form and Figure	Color Application	Life Symbolism
		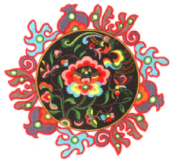	
Symmetry	Naive charm	Cross-stitch	Heritage
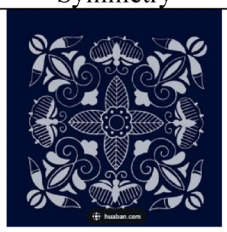			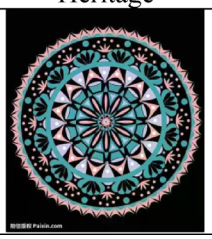

Table 6. Summary of stylistic feature factors.

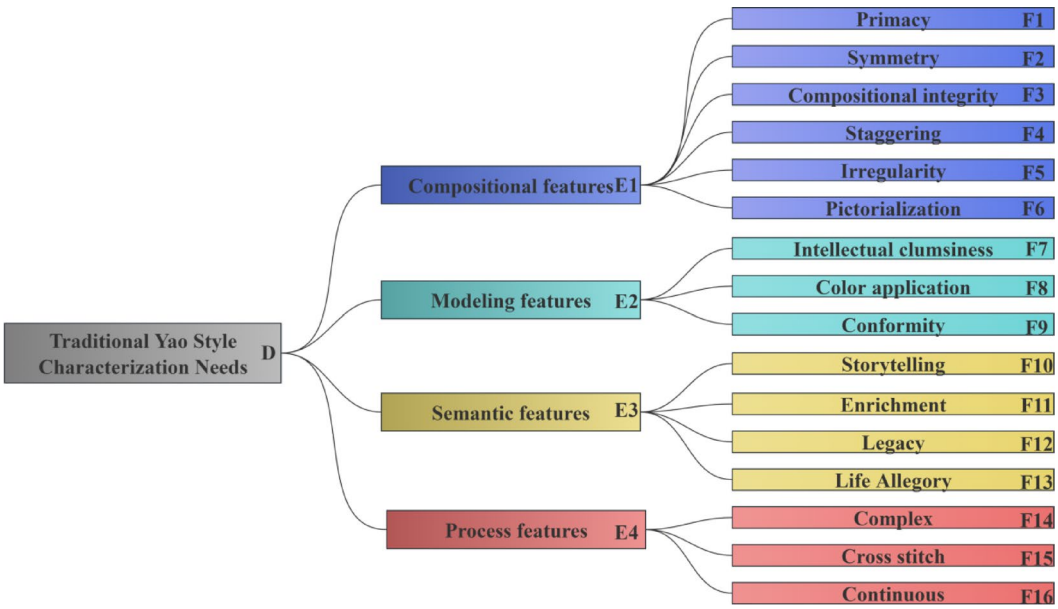

Fig. 11. shows the demand levels of Miao ethnic style characteristics.

Following the stylistic feature model presented in Fig. 7, the calculation procedures outlined in steps (1) and (2) were repeated to determine the weight of each factor for the Miao ethnic group's traditional stylistic features. A fuzzy consistency test was subsequently conducted. Fuzzy judgment matrices were constructed for each criterion level. The primary factor scores and the resulting fuzzy judgment matrices for calculations $E1$ through $E4$ are presented below.

$$\mathrm{A}=\begin{array}{c} \\ E1 \\ E2 \\ E3 \\ E4 \end{array}\begin{array}{c} \begin{array}{cccc} E1 & E2 & E3 & E4 \end{array} \\ \begin{bmatrix} 0.5 & 0.8 & 0.6 & 0.7 \\ 0.2 & 0.5 & 0.4 & 0.4 \\ 0.4 & 0.6 & 0.5 & 0.7 \\ 0.3 & 0.3 & 0.3 & 0.5 \end{bmatrix} \end{array} \quad w=\begin{array}{c} \\ E1 \\ E2 \\ E3 \\ E4 \end{array}\begin{bmatrix} 0.35 \\ 0.1667 \\ 0.2833 \\ 0.2 \end{bmatrix}$$

Construct a fuzzy judgment matrix for each sub-criterion level, and derive the matrix score and weight calculation results for $E1$ as follows:

$$E=\begin{array}{c} \\ F1 \\ F2 \\ F3 \\ F4 \\ F5 \\ F6 \end{array}\begin{array}{c} \begin{array}{cccccc} F1 & F2 & F3 & F4 & F5 & F6 \end{array} \\ \begin{bmatrix} 0.5 & 0.2 & 0.3 & 0.6 & 0.6 & 0.4 \\ 0.8 & 0.5 & 0.6 & 0.7 & 0.7 & 0.6 \\ 0.7 & 0.4 & 0.5 & 0.7 & 0.7 & 0.6 \\ 0.4 & 0.3 & 0.3 & 0.5 & 0.4 & 0.3 \\ 0.4 & 0.3 & 0.3 & 0.6 & 0.5 & 0.4 \\ 0.6 & 0.4 & 0.4 & 0.6 & 0.6 & 0.5 \end{bmatrix} \end{array} \quad w=\begin{array}{c} \\ F1 \\ F2 \\ F3 \\ F4 \\ F5 \\ F6 \end{array}\begin{bmatrix} 0.14 \\ 0.2267 \\ 0.2067 \\ 0.1133 \\ 0.1333 \\ 0.18 \end{bmatrix}$$

Construct a fuzzy judgment matrix for each sub-criterion level, and derive the matrix score and weight calculation results for $E2$ as follows:

$$E=\begin{array}{c} \\ F7 \\ F8 \\ F9 \end{array}\begin{array}{c} \begin{array}{ccc} F7 & F8 & F9 \end{array} \\ \begin{bmatrix} 0.5 & 0.4 & 0.3 \\ 0.6 & 0.5 & 0.4 \\ 0.7 & 0.6 & 0.5 \end{bmatrix} \end{array} \quad w=\begin{array}{c} \\ F7 \\ F8 \\ F9 \end{array}\begin{bmatrix} 0.2333 \\ 0.3333 \\ 0.4333 \end{bmatrix}$$

Construct a fuzzy judgment matrix for each sub-criterion level, and derive the matrix score and weight calculation results for $E3$ as follows:

$$E=\begin{array}{c} \\ F10 \\ F11 \\ F12 \\ F13 \end{array}\begin{array}{c} \begin{array}{cccc} F10 & F11 & F12 & F13 \end{array} \\ \begin{bmatrix} 0.5 & 0.6 & 0.6 & 0.4 \\ 0.4 & 0.5 & 0.6 & 0.3 \\ 0.4 & 0.4 & 0.5 & 0.4 \\ 0.6 & 0.7 & 0.6 & 0.5 \end{bmatrix} \end{array} \quad w=\begin{array}{c} \\ F10 \\ F11 \\ F12 \\ F13 \end{array}\begin{bmatrix} 0.2667 \\ 0.2167 \\ 0.2 \\ 0.3167 \end{bmatrix}$$

Construct a fuzzy judgment matrix for each sub-criterion level, and derive the matrix score and weight calculation results for $E4$ as follows:

$$E=\begin{array}{c} \\ F14 \\ F15 \\ F16 \end{array}\begin{array}{c} \begin{array}{ccc} F14 & F15 & F16 \end{array} \\ \begin{bmatrix} 0.5 & 0.2 & 0.4 \\ 0.8 & 0.5 & 0.6 \\ 0.6 & 0.4 & 0.5 \end{bmatrix} \end{array} \quad w=\begin{array}{c} \\ F14 \\ F15 \\ F16 \end{array}\begin{bmatrix} 0.2 \\ 0.4667 \\ 0.3333 \end{bmatrix}$$

The CR values for features D, $E1$, $E2$, $E3$, and $E4$ are 0.0225, 0.0438, 0.0432, 0.0222, and 0.0222 respectively, all less than 0.1, passing the one-tailed test. Multiplying the primary weight values by the secondary weight values yields the composite weight values for Miao ethnic style features. These composite weights are then ranked, as shown in Table 7.

###The calculation of weight values for Miao ethnic style characteristics enables designers to concentrate on high-weight stylistic patterns. This approach improves design process efficiency and provides deeper insight into consumers' core perceptual needs regarding traditional motifs.

Based on this analysis, eight style characteristics with weights exceeding 0.6 were selected for the subsequent construction of the relationship matrix.

Core design feature extraction based on FQFD

Design morphology deconstruction

In affective engineering, morphological decomposition represents a pivotal methodology. It involves analyzing the structure and form of products or systems to reveal the intrinsic connections between affective imagery and physical design attributes [32–34]. This approach is user-centered, emphasizing the systematic analysis of how design elements (e.g., form, color, materials) influence user emotions and cognition, based on user perception and experience.

	Cross-stitch	Life meaning	Symmetry	Story-telling	Concrete form	Continuity	Pictographic	Richness
Weight	0.0933	0.0897	0.0793	0.0756	0.0722	0.0667	0.063	0.0614

Table 7. Weight of miao ethnic style features.

The core premise of morphological decomposition involves deconstructing a product into its constituent parts to analyze the form, structure, and function of each element. This process encompasses not only the physical components but also design language, structural relationships, color schemes, and material selection. Through systematic decomposition, designers can acquire a deeper understanding of the intrinsic logic and sensory attributes of a product or system. This facilitates more accurate insights into user needs, reduces development risks, and improves product-market fit .

In this study, a panel of industrial design experts was assembled to conduct a morphological decomposition analysis on a collection of 100 smart home fan images. Through a systematic evaluation, six primary morphological elements were identified: fan guard, fan blades, support frame, fan base, indicator panel, and voice port. Based on this decomposition, ten distinct design archetypes were derived, as illustrated in Fig. 12.

Calculation of design feature weights

During the construction of the House of Quality (HOQ) for the Fuzzy Quality Function Deployment (FQFD) process, the six categories of smart home fan design features were positioned as the "Hows" (technical requirements) in the ceiling of the matrix. Concurrently, the top nine user emotional needs, along with their corresponding weight values, were placed as the "Whats" (customer attributes) on the left wall of the HOQ.

	Fan-guard	Fan-blade	Fan-bracket	Fan-base	Indicating lamp	Sound
Style1						
Style2						
Style3						
Style4						
Style5						
Style6						
Style7						
Style8						
Style9						
Style10						

Fig. 12. Design features of the smart fan.

	Weight of emotional needs	Fan cover	Fan blades	Bracket	Fan base	Indicator light	Voice hole
Intelligent C2	0.0737	(3, 5, 7)	(7, 9, 9)	(5, 7, 9)	(7, 9, 9)	(7, 9, 9)	(1, 1, 3)
Practical C3	0.0652	(5, 7, 9)	(7, 9, 9)	(7, 9, 9)	(7, 9, 9)	(7, 9, 9)	(7, 9, 9)
Safe C6	0.0867	(7, 9, 9)	(3, 5, 7)	(7, 9, 9)	(7, 9, 9)	(3, 5, 7)	(7, 9, 9)
Humanized C9	0.0889	(3, 5, 7)	(1, 1, 3)	(7, 9, 9)	(1, 1, 3)	(7, 9, 9)	(1, 1, 3)
Warm C10	0.1056	(3, 5, 7)	(1, 1, 3)	(5, 7, 9)	(1, 1, 3)	(1, 3, 5)	(1, 1, 3)
Unique C11	0.0778	(5, 7, 9)	(1, 3, 5)	(5, 7, 9)	(3, 5, 7)	(7, 9, 9)	(1, 1, 3)
Natural C12	0.0611	(7, 9, 9)	(7, 9, 9)	(3, 5, 7)	(1, 3, 5)	(1, 3, 5)	(7, 9, 9)
Small C13	0.0489	(7, 9, 9)	(5, 7, 9)	(3, 5, 7)	(1, 3, 5)	(1, 3, 5)	(3, 5, 7)
Comfortable C15	0.0733	(5, 7, 9)	(7, 9, 9)	(5, 7, 9)	(3, 5, 7)	(1, 3, 5)	(3, 5, 7)
Comprehensive weight	13.5	10.8	14.6	9.9	11.5	8.9	
Relative weight	0.19	0.16	0.21	0.14	0.17	0.13	

Table 8. Quality house of design features for home smart fans.

	Weight of emotional needs	Cross-stitch F15	Life meaning F13	Symmetry F2	Story-telling F10	Concrete form F9	Continuity F16	Pictographic F6	Richness F11
Intelligent C2	0.0737	(3, 5, 7)	(7, 9, 9)	(5, 7, 9)	(7, 9, 9)	(7, 9, 9)	(1, 1, 3)	(7, 9, 9)	(3, 5, 7)
Practical C3	0.0652	(5, 7, 9)	(7, 9, 9)	(7, 9, 9)	(1, 1, 3)	(7, 9, 9)	(7, 9, 9)	(1, 1, 3)	(3, 5, 7)
Safe C6	0.0867	(7, 9, 9)	(3, 5, 7)	(7, 9, 9)	(7, 9, 9)	(3, 5, 7)	(7, 9, 9)	(1, 1, 3)	(5, 7, 9)
Humanized C9	0.0889	(3, 5, 7)	(1, 1, 3)	(7, 9, 9)	(1, 1, 3)	(7, 9, 9)	(1, 3, 5)	(7, 9, 9)	(5, 7, 9)
Warm C10	0.1056	(3, 5, 7)	(1, 1, 3)	(5, 7, 9)	(1, 1, 3)	(1, 3, 5)	(3, 5, 7)	(5, 7, 9)	(7, 9, 9)
Unique C11	0.0778	(5, 7, 9)	(1, 3, 5)	(5, 7, 9)	(3, 5, 7)	(7, 9, 9)	(3, 5, 7)	(1, 1, 3)	(1, 1, 3)
Natural C12	0.0611	(3, 5, 7)	(3, 5, 7)	(7, 9, 9)	(1, 1, 3)	(1, 3, 5)	(7, 9, 9)	(1, 3, 5)	(1, 1, 3)
Small C13	0.0489	(7, 9, 9)	(3, 5, 7)	(7, 9, 9)	(3, 5, 7)	(3, 5, 7)	(7, 9, 9)	(3, 5, 7)	(3, 5, 7)
Comfortable C15	0.0733	(7, 9, 9)	(3, 5, 7)	(7, 9, 9)	(3, 5, 7)	(3, 5, 7)	(7, 9, 9)	(3, 5, 7)	(3, 5, 7)
Comprehensive weight	13.1	9.2	16	8.6	12.3	12.2	9.8	10.9	
Relative weight	0.14	0.10	0.17	0.09	0.13	0.13	0.11	0.12	

Table 9. Miao ethnic style characteristic quality house.

This configuration enables a systematic analysis of the relationships between design features and user emotional needs.

This mapping model helps designers identify the core design features that most significantly influence user perception, thereby streamlining the design process and enhancing development efficiency [35,36]. The complete structure of the HOQ mapping emotional needs to design features for the smart home fan is presented in Table 8.

Finally, based on Table 8, we selected the top four categories of design features to incorporate into the subsequent sentiment prediction matrix.

Calculation of style feature weights

Similarly, the top nine selected emotional vocabulary terms and their corresponding weights are positioned as the "Whats" (customer attributes) on the left wall of the FQFD House of Quality (HOQ). This allows for a systematic analysis of the correlations between user emotional needs and Miao ethnic style characteristics.

This methodology enables designers to accurately identify Miao-style features that align with user emotional preferences, thereby establishing a foundation for subsequent design implementation. The HOQ that maps the relationship between user emotional needs and Miao ethnic style characteristics for smart home fans is presented in Table 9.

Generating and coding design variants

To systematically explore the design space for smart home fans and provide ample training and testing data for the emotional prediction model in this study, we employed a morphological matrix combined with parametric combination methods based on the deconstructed morphological elements. This approach generated a large-scale set of virtual design variants. The specific generation process is as follows:

Step 1: Constructing the Morphological Matrix: Based on the morphological deconstruction outlined in Section "Design morphology deconstruction", we systematically organized six core morphological elements (fan cover, fan blades, bracket, fan base, indicator panel, voice port) and their 10 design style variants into a morphological matrix. Theoretically, this matrix can generate 10 (fan cover) × 10 (fan blades) × 10 (support frame) × 10 (fan base) × 10 (control panel) × 10 (speaker grille) = 10^6 potential combinations.

Step 2: Feasibility Screening and Combination Reduction: Recognizing that not all theoretical combinations are feasible from an engineering or aesthetic perspective, we engaged a panel of three industrial design experts

for preliminary evaluation. Experts eliminated obviously implausible designs based on design principles (e.g., structural stability, stylistic harmony)—such as pairing an ultra-minimalist bracket with an overly complex, heavy base. Following this step, we selected 30,000 visually and conceptually coherent, feasible designs for subsequent emotional prediction.

Step 3: Digital Encoding of Design Concepts: Each generated virtual design was converted into a feature vector for model processing. This vector comprised six discrete categorical variables, each representing a specific stylistic variant (valued 1–10) adopted for a morphological element. For example, a design could be encoded as [1–3,5,7,9], denoting its use of a 3rd-category fan cover, 7th-category fan blades, 2nd-category stand, and so on.

Through this approach, we systematically defined and enumerated a virtual design space containing tens of thousands of feasible points. This ensures the CPO-CNN-LSSVM model can learn and predict across a broad, continuous design spectrum, identifying optimal emotional design combinations beyond the initial 100 limited samples. Similarly, the Miao ethnic pattern feature combinations were constructed using this methodology.

Product emotional data prediction based on CPO-CNN-LSSVM

Dataset construction

To evaluate product form characteristics effectively, a panel of 278 evaluators was recruited, comprising 28 experienced designers (10.1%), 90 industrial design professors (32.4%), and 160 industrial design students (57.5%). A Kendall's W coefficient test demonstrated an inter-rater reliability of 0.89 ($p < 0.001$), indicating a high level of consistency in the evaluation outcomes.

The three simplified emotional design dimensions—"Intelligent Stability," "Emotional Comfort," and "Harmonious Charm"—were adopted as the primary evaluation metrics. The evaluators conducted emotional assessments on 200 sample smart fans to build the foundational dataset. Simultaneously, morphological coding was performed on all samples. The four most prevalent morphological features—stand, fan guard, indicator panel, and fan blades—were selected and integrated into a mapping matrix with the emotional dimensions (Table 10) to enable a systematic analysis of the relationships between morphological characteristics and users' emotional perceptions.

The CPO-CNN-LSSVM hybrid model was employed to investigate the complex, nonlinear relationship between the design features of innovative fan products and users' emotional perceptions. During the modeling phase, the input features consisted of design feature scores from 200 smart fan product samples after morphological coding. The output response was the average scores assigned by evaluators across three affective dimensions—"Intelligent Stability," "Comforting Emotion," and "Pleasant Rhythm"—for each sample. Adhering to a consistent data partitioning strategy, the 200 samples were randomly allocated into a training set (120 samples, 60%) and a test set (80 samples, 40%). The randomization process employed stratified sampling to ensure distributional similarity between training and test sets on key features (e.g., affective dimension scores), thereby minimizing partitioning bias. Given the limited sample size, cross-validation could introduce excessive computational overhead and deviate from the study's objective (evaluating model performance on an independent test set). Therefore, a fixed partitioning approach was adopted, though model robustness was validated via Bootstrap resampling (as detailed in Section "Model Performance Validation"). This methodology successfully constructed a predictive model that effectively maps intelligent fan design features to user emotional perceptions [37]. All modeling and computational processes were completed in the MATLAB 2024b software environment. The hardware configuration consisted of an Intel i7-14700KF processor and an NVIDIA GeForce RTX 3060 Ti graphics card (8 GB VRAM), running on the Windows 11 operating system.

Parameter setting analysis and sample size adaptive validation

Compared to other optimization algorithms, CPO distinguishes itself through its structural simplicity, robust global exploration capability (enabling compelling exploration of the extensive search space to avoid local

	Bracket	Fan Cover	Control Panel	Fan Blade	Smart Stabilization	Comfort	Harmony
1	8	9	7	8	8.8	7.5	8
2	8.2	8.8	7.2	8.3	8.2	8	7
3	9	9	8	7	8.8	7.5	8.2
4	9	9.4	9	9	9	7.5	7.9
5	8	8	9	7	8.8	7	8.5
6	7	9	8	8	8.2	7	8.2
7	3	9	9	8	8	7.6	8.4
…	…	…	…	…	…	…	…
195	8	8	7	7	7.9	7	7.5
196	9	8.7	7	7	7.9	7.5	8.5
197	8	8	7.9	7.9	7.8	7.4	8
198	3	8	9	7	7	7	8
199	8	8	9	7	7	7	8.5
200	9	8	8	7	7.9	7	8

Table 10. Matrix for mapping interior features to user emotions.

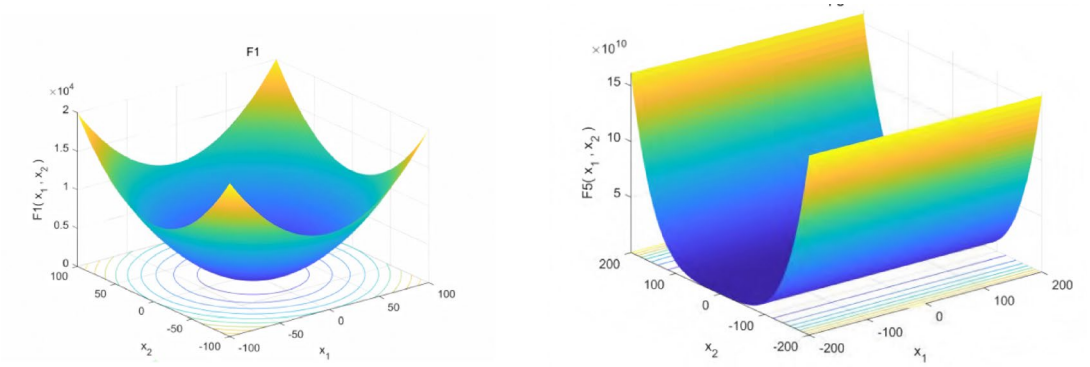

(a)F1 test function (b)F5 test function

Fig. 13. F1 and F5 test functions.

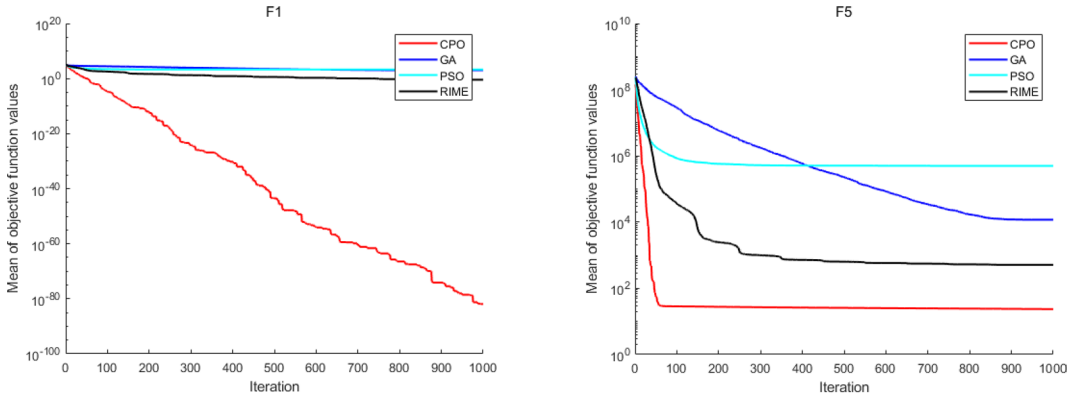

(a)F1 convergence curve (b)F5 convergence curve

Fig. 14. F1 and F5 convergence curves.

minima), a population diversity maintenance strategy based on a novel cyclic population reduction mechanism, and significant convergence acceleration during the late stages of the optimization process.

To validate CPO's performance, this paper conducts comparative experiments using 23 standard benchmark functions. The experiments evaluate CPO alongside widely used algorithms: Particle Swarm Optimization (PSO), Rime Optimization Algorithm (RIME), and Genetic Algorithm (GA). PSO relies on the cooperative behavior of particle swarms to balance global and local search for optimal parameter identification. However, in high-dimensional hyperparameter optimization, PSO faces challenges in avoiding local optima, particularly when the search space is complex, limiting its global search capability. RIME simulates natural processes by dynamically adjusting the diffusion and aggregation of ice crystal particles, effectively maintaining population diversity and preventing premature convergence. However, RIME converges relatively slowly, especially in the later stages of parameter search, where its incremental convergence mechanism may increase optimization time. GA simulates natural selection and the increase in fitness in biological evolution. Through operations like selection, crossover, and mutation, it continuously optimizes population fitness to obtain the optimal solution ultimately. However, in high-dimensional hyperparameter optimization, GA typically requires more iterations than CPO to reach the optimal solution.

All algorithms share uniform parameter settings: a maximum iteration count of 1000 and a population size of 50. Selected experimental results are shown in Figs. 13–14, where Fig. 13 displays convergence curves for the F1 and F5 functions, and Fig. 14 compares the performance of different optimization methods on these two test functions.

Based on the experimental results presented above, the convergence curves for the F1 and F5 evaluation metrics in Fig. 16 demonstrate that the CPO algorithm exhibits superior optimization performance compared to other optimization algorithms. It demonstrates significant advantages during hyperparameter optimization, particularly in terms of global search capability, convergence speed, and stability. Through rapid iteration, CPO can locate optimal solutions within fewer iterations while effectively avoiding overfitting and underfitting.

Before applying CPO for automatic optimization of the CPO-CNN-LSSVM model, the basic architecture and training configuration must be predefined. These structural parameters are typically excluded from the optimization process and must be manually set through preliminary experiments. Key structural elements for

Phase	Component Category	Candidate Configuration	Validation RMSE	Training Stability
Phase I (Kernel Size)	Convolutional Kernel Size	3×3	0.161	High
		5×5	0.164	Medium
		7×7	0.175	Low
Phase II (Pooling Strategy)	Pooling Method	Max Pooling	0.159	High
		Average Pooling	0.164	High
		Stochastic Pooling	0.172	Medium
Phase III (Activation Function)	Activation Function	ReLU	0.158	High
		Sigmoid	0.165	Medium
		Tanh	0.162	Medium

Table 11. Detailed performance comparison of CNN-LSSVM basic components in a multi-stage experiment.

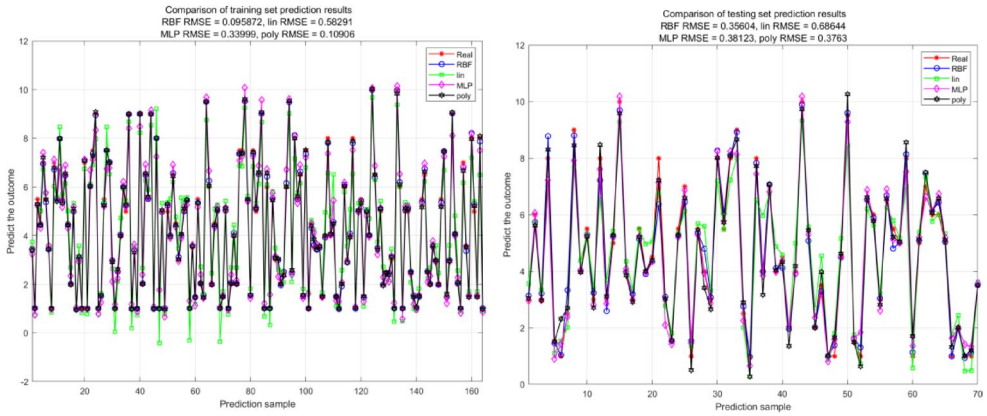

Fig. 15. Performance comparison of kernel functions.

the CNN component include convolution kernel size, pooling method, and activation function type; while the LSSVM component requires presetting kernel function type and objective function form. To scientifically determine these configurations, we conducted comparative experiments on the CNN component, with results shown in Table 11. The experiments demonstrate that using the ReLU activation function achieves the lowest RMSE on the validation set and the highest training stability. Regarding LSSVM kernel function validation, Fig. 15 indicates that selecting the RBF kernel achieves the lowest RMSE.

The core mechanism of the CPO-CNN-LSSVM model lies in treating the CPO-CNN module as a powerful feature extractor that maps raw input data into a high-dimensional, linearly separable feature space. Subsequently, LSSVM performs the final efficient classification or regression within this space. This architecture ingeniously combines the strengths of CNN in feature learning with LSSVM's exceptional generalization performance on small samples.

Within this optimized framework, the primary control parameters in the CPO algorithm are the defense probability (Pd), fitness value (α), and population diversity (γ). Through sensitivity analysis experiments (orthogonal experimental design) on parameters like Pd in the CPO algorithm to determine optimal biological behavior probability and perceptual weight, we found that Pd = 0.7, $\alpha = 0.55$, and pop = 50 yield the fastest convergence, highest accuracy, and best diversity, as shown in Table 12.

Through range analysis, we further quantified the impact of each parameter on performance metrics. The results revealed significant variations in the influence of different parameters across performance indicators. As shown in Table 13, the defense probability (Pd) exerted the most pronounced effect on algorithm performance, consistent with its crucial role in balancing exploration and exploitation within the Crown Porcupine Algorithm. The perception weight α follows in importance, while the population size has a relatively minor impact; however, it still requires a reasonable configuration in practical applications.

Based on the Pareto Front multi-objective optimization analysis method, we selected the optimal configuration scheme that simultaneously optimizes convergence speed and accuracy. Pareto analysis identifies the optimal balance point among multiple conflicting objectives, ensuring the selected parameter configuration achieves high performance across all aspects. The final optimal parameter configuration is: Perception weighting α:β:γ = 0.55:0.30:0.15 (the optimized weighting ratio enhances information utilization efficiency); Population size pop: 50 (this size achieves an optimal balance between computational efficiency and search effectiveness). This configuration significantly improves the algorithm's convergence speed and solution quality while maintaining population diversity.

We validated the effectiveness of the CPO algorithm's optimization by analyzing the dynamic trajectories of LSSVM hyperparameters during the optimization process. As shown in Fig. 16, the regularization parameter γ

Pd	α	pop	Convergence Iteration	Optimal RMSE	Population Diversity Entropy
0.5	0.4	20	95	0.152	0.76
0.5	0.5	30	88	0.148	0.78
0.5	0.6	50	92	0.151	0.75
0.6	0.4	30	82	0.145	0.81
0.6	0.5	50	78	0.143	0.84
0.6	0.6	20	85	0.147	0.79
0.7	0.4	50	75	0.142	0.86
0.7	0.5	20	80	0.144	0.82
0.7	0.6	50	72	0.138	0.88

Table 12. Detailed results of orthogonal experiment for CPO parameters.

Parameter	onvergence Algebraic Deviation	Optimal RMSE Deviation	Diversity Entropy Deviation	Comprehensive Impact Weight	Sensitivity Ranking
Pd	23.3	0.015	0.16	0.42	1
α	18.7	0.012	0.13	0.33	2
pop	15.2	0.009	0.11	0.25	3

Table 13. Detailed results of parameter range analysis.

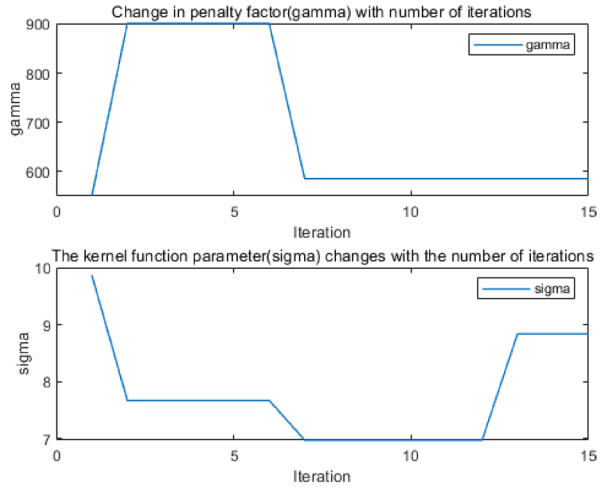

Fig. 16. Iteration of kernel function with penalty factor.

and the RBF kernel parameter σ exhibit clear and reasonable evolutionary patterns with the number of iterations: γ converges rapidly to around 7.5 within the initial iterations (within 10 generations), demonstrating excellent rapid parameter positioning capability; simultaneously, σ exhibits a monotonically decreasing trend, ultimately stabilizing at 8.5. This optimization process demonstrates that the CPO algorithm efficiently coordinates model complexity (controlled by γ) with feature mapping relationships (controlled by σ), enabling LSSVM to maintain sufficient data feature fitting capability while avoiding overfitting.

Finally, to systematically validate the training effectiveness and generalization capability of the CPO-CNN-LSSVM model under limited sample sizes, we designed a progressive sample size performance test. By randomly sampling training subsets of varying sizes (40–160 samples), we evaluated the model's performance changes on a fixed test set (80 samples). The experimental results are shown in Table 14, and the performance trends are illustrated in Fig. 17.

Analysis indicates that when the training sample size increases from 40 to 120, model performance improves rapidly and stabilizes: the test set RMSE decreases significantly from 0.038 to 0.016 (a 57.9% reduction). In comparison, R^2 increases from 0.950 to 0.988 (a 4.0% increase). Crucially, when the sample size increased further from 120 to 160, the performance improvement became negligible (RMSE improved by only 0.001, R^2 increased by 0.004), indicating that 120 training samples had brought the model's performance close to its convergence limit. Furthermore, the training-to-test performance gap—a key metric for overfitting—consistently narrowed with increasing sample size, decreasing from 74.1% at 40 samples to 14.3% at 120 samples. This fully validates

Training Samples	Training RMSE	Test RMSE	Training R^2	Test R^2	Overfitting Gap (%)	Training Time (s)
40	0.022	0.038	0.983	0.950	74.1	40
60	0.019	0.028	0.987	0.973	47.4	60
80	0.017	0.022	0.989	0.981	29.4	80
100	0.015	0.019	0.991	0.985	26.7	100
120	0.014	0.016	0.992	0.988	14.3	120
140	0.013	0.015	0.993	0.990	15.4	140
160	0.013	0.015	0.993	0.992	15.4	160

Table 14. Performance comparison under different training sample sizes.

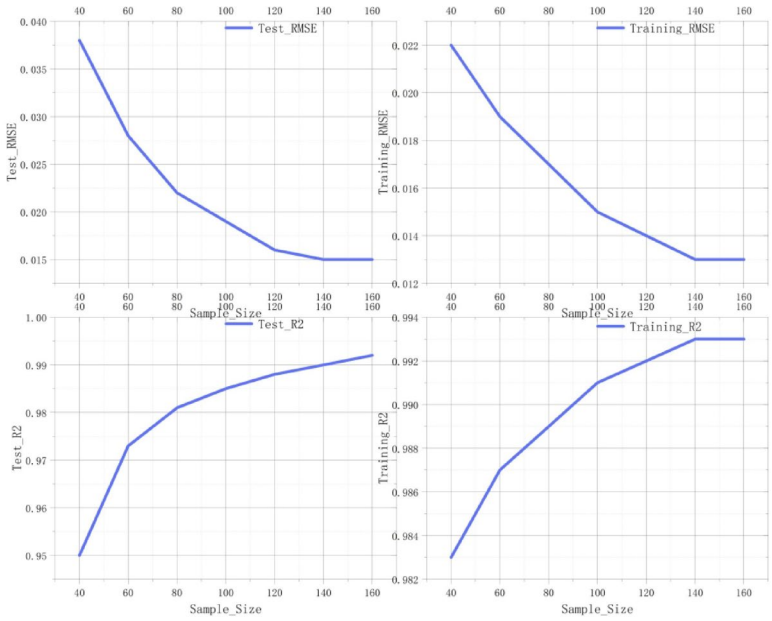

Fig. 17. Performance testing.

that our minimalist CNN architecture and CPO regularization strategy jointly ensure the model's exceptional generalization capability under small-sample conditions.

In summary, combining the minimalist CNN architecture design (total parameters: 6,240; parameter-to-sample ratio: 52.0) with the above systematic validation results confirms that 120 training samples are sufficient to train the CPO-CNN-LSSVM model fully. This enables it to achieve near-optimal predictive performance, fully meeting the design prediction requirements of this study.

Experimental results

During the prediction process, the dataset for the "Zhiwen" dimension was preprocessed by first normalizing the raw data to mitigate the influence of scale differences on model training. The data matrix was then transposed to conform to the input structure required by the CPO-CNN-LSSVM model. The model parameter settings utilized the results from the parameter analysis conducted during the preliminary experimental phase.

The trend of the optimal fitness value during model training is shown in Fig. 18. The upper curve, representing the Root Mean Square Error (RMSE), exhibits a high error during the initial phase (generations 0–25), indicating that the model had not yet effectively learned to extract data features. Between generations 25 and 40, the RMSE decreased rapidly, which indicates a significant improvement in the model's learning capability. After generation 40, the curve stabilized, suggesting that the model had converged to an optimal state. The lower loss curve shows that both the training loss (blue) and validation loss (orange) converge after epoch 40, demonstrating the model's strong generalization capability. The training process validates the effectiveness of the CPO algorithm for feature optimization and confirms the proficiency of the CNN in feature extraction.

The optimized features were subsequently used as input to the LSSVM for training. The model's performance was evaluated on test sets representing three user types, as detailed in Fig. 19. The overall linear fitting results, presented in Fig. 20, demonstrate that the CPO-CNN-LSSVM model establishes a robust mapping relationship between innovative fan design features and user affective factors.

In comparison to other optimization algorithms, the proposed CPO-CNN-LSSVM model demonstrates several distinct advantages. The model's strengths are primarily manifested in its feature extraction and

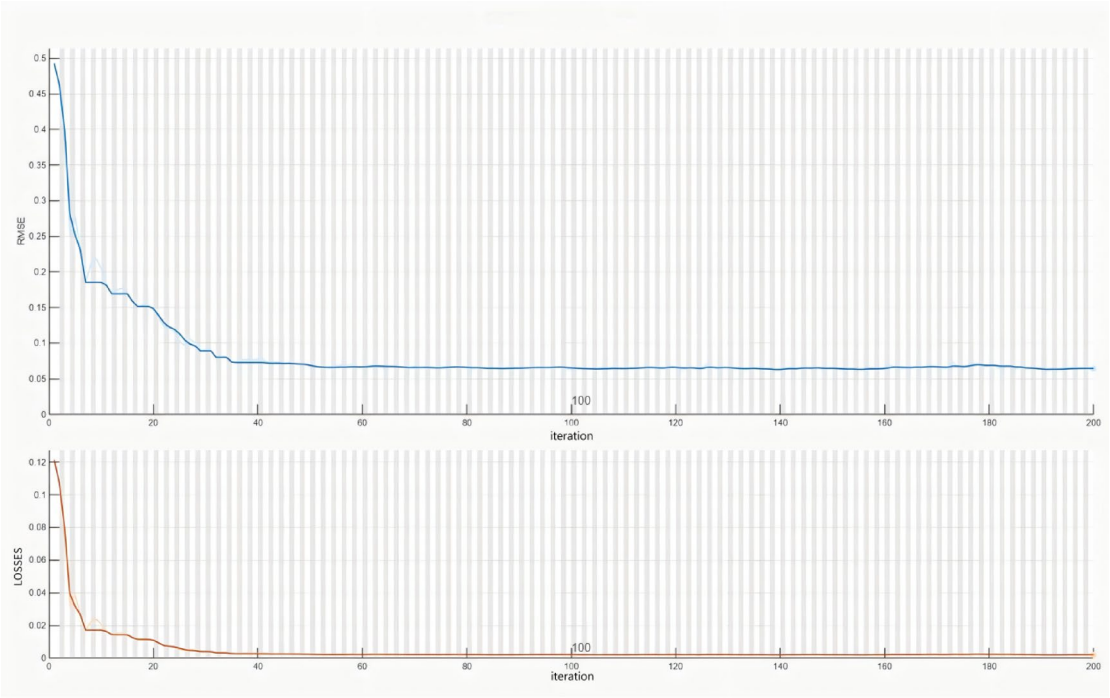

Fig. 18. CPO-CNN-LSSVM model iterative process.

optimization capabilities. The CNN component automatically captures local correlations and spatial hierarchical features in the data, thereby providing high-quality feature representations for subsequent regression analysis [38]. Building on this, the Least Squares Support Vector Machine (LSSVM) component leverages its convex optimization properties [39] to ensure convergence to a global optimum, thereby effectively mitigating the risk of local optima. Furthermore, by minimizing structural risk, the LSSVM endows the model with excellent generalization capability and robustness, enabling it to maintain stable performance even with limited data or in the presence of noise.

A critical advantage is the integration of the Crested Porcupine Optimizer (CPO), which automates the hyperparameter optimization process. The CPO algorithm employs adaptive search strategies to identify optimal configurations for both CNN architectures and LSSVM kernel parameters, thereby significantly reducing the reliance on manual tuning and enhancing model reproducibility and usability [40].

This integrated, end-to-end optimization framework not only maximizes model performance but is particularly well-suited for industrial regression problems requiring high accuracy and stability, owing to its efficient training speed and strong noise resistance. Thus, it provides a reliable solution for modeling complex nonlinear relationships.

Figure 20, the horizontal axis (x-axis) represents the actual observed values, the vertical axis (y-axis) represents the model-predicted values, and the purple line denotes the ideal fit ($y=x$). This scatter plot with a fitted line provides a visual representation of the model's goodness of fit. The model's coefficient of determination (R^2) consistently exceeded 0.9 across predictions, approaching a value of 1, which indicates excellent fit and explains the vast majority of the variance in the sample data [41,42]. Similarly, the root mean square error of prediction (RMSEP) remained consistently low, further validating the model's high predictive accuracy. Figure 15 demonstrates that most data points (blue) are clustered closely around the ideal fit line, indicating high predictive accuracy for the majority of samples.

Using the fully trained CPO-CNN-LSSVM model, four new design feature combinations were introduced, and emotional prediction values were generated for 30,000 smart fan design variants. Among these, Design Combination #1768 achieved the highest predicted user emotional rating (8.45). This result not only provides data-driven support for the creative design of smart fans but also validates the effectiveness and practical value of the CPO-CNN-LSSVM model in industrial design and engineering applications.

Emotional data prediction for traditional patterns based on CPO-CNN-LSSVM

Dataset construction

To systematically analyze the nonlinear relationship between Miao ethnic style characteristics and product design, a panel of 150 evaluators was recruited. The panel comprised 28 experienced designers, 30 industrial design professors, 30 graphic design professors, and 22 Miao intangible cultural heritage inheritors. A Kendall's W coefficient test indicated a high inter-rater reliability of 0.89 ($p<0.001$), demonstrating strong consistency in the evaluation outcomes.

Affective evaluations were conducted on 200 smart fan product samples using a 1–5 point scale across four design characteristics, thereby constructing the foundational dataset. Subsequently, morphological coding was

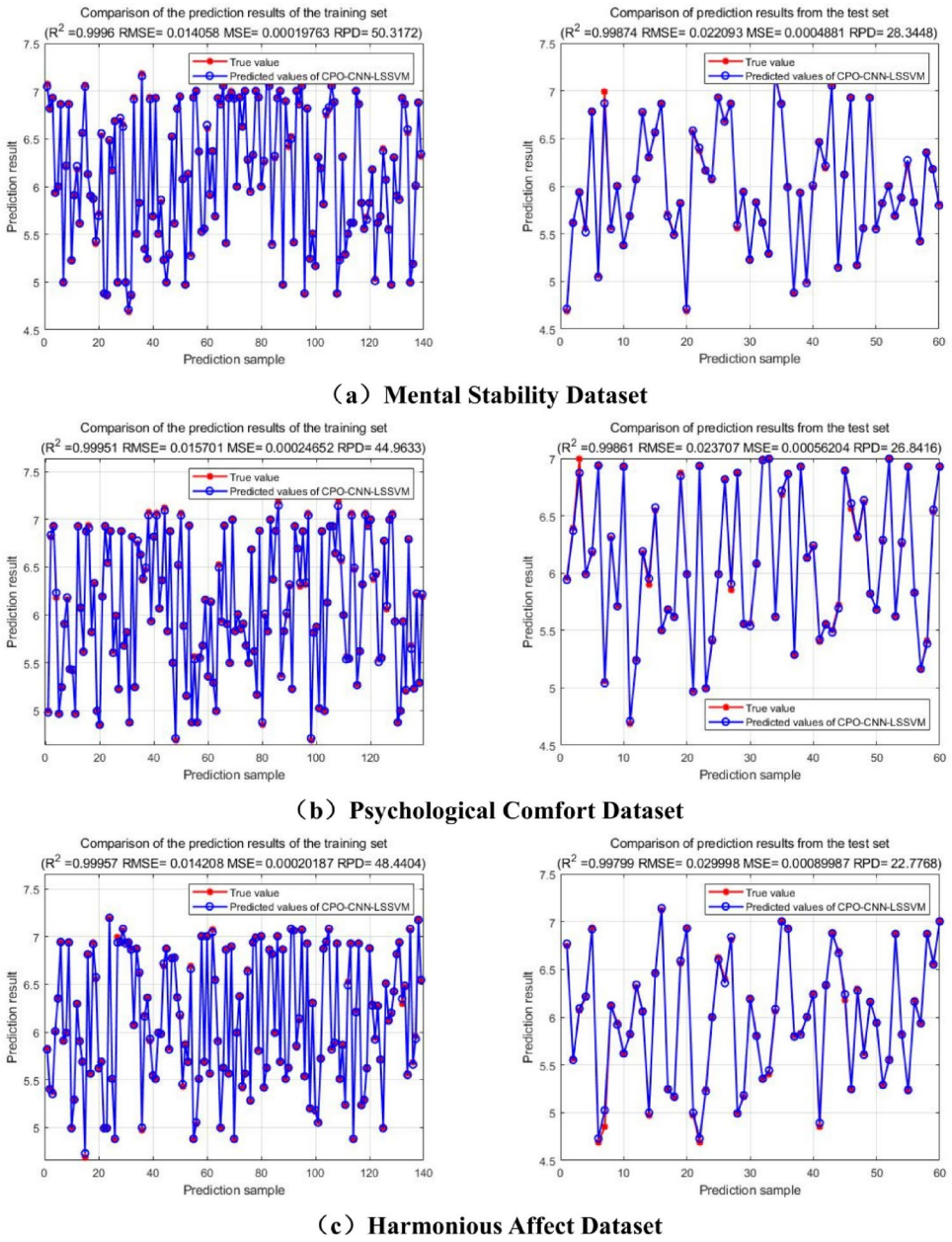

Fig. 19. Performance Evaluation of the CPO-CNN-LSSVM Model on the User Sentiment Dataset. **a** to **c** Performance comparison between the training and testing sets for the Mental Stability, Psychological Comfort, and Harmonious Affect datasets.

performed, which identified the eight most prevalent Miao-style features: Cross-Stitch (F15), Meaning of Life (F13), Symmetry (F2), Narrativity (F10), Figurative Form (F9), Continuity (F16), Pictographic Symbols (F6), and Richness (F11). These features were then integrated with the affective evaluation data into a mapping matrix (Table 15) to systematically analyze the complex relationships between stylistic features and user perceptions.

The established CPO-CNN-LSSVM model architecture was further employed to investigate the complex mapping relationship between Miao ethnic style features and innovative fan product design characteristics. For this phase, the input features consisted of the encoded scores for 200 Miao-style features. The output responses were defined as the evaluators' average ratings for the three emotional dimensions: "Intelligent Stability," "Emotional Comfort," and "Harmonious Charm."

Consistent with the previous data partitioning strategy, the first 120 samples were allocated to the training set, and the remaining 80 samples constituted the test set. This methodology successfully produced a predictive model that effectively represents the nonlinear relationship between Miao ethnic style features and product design characteristics.

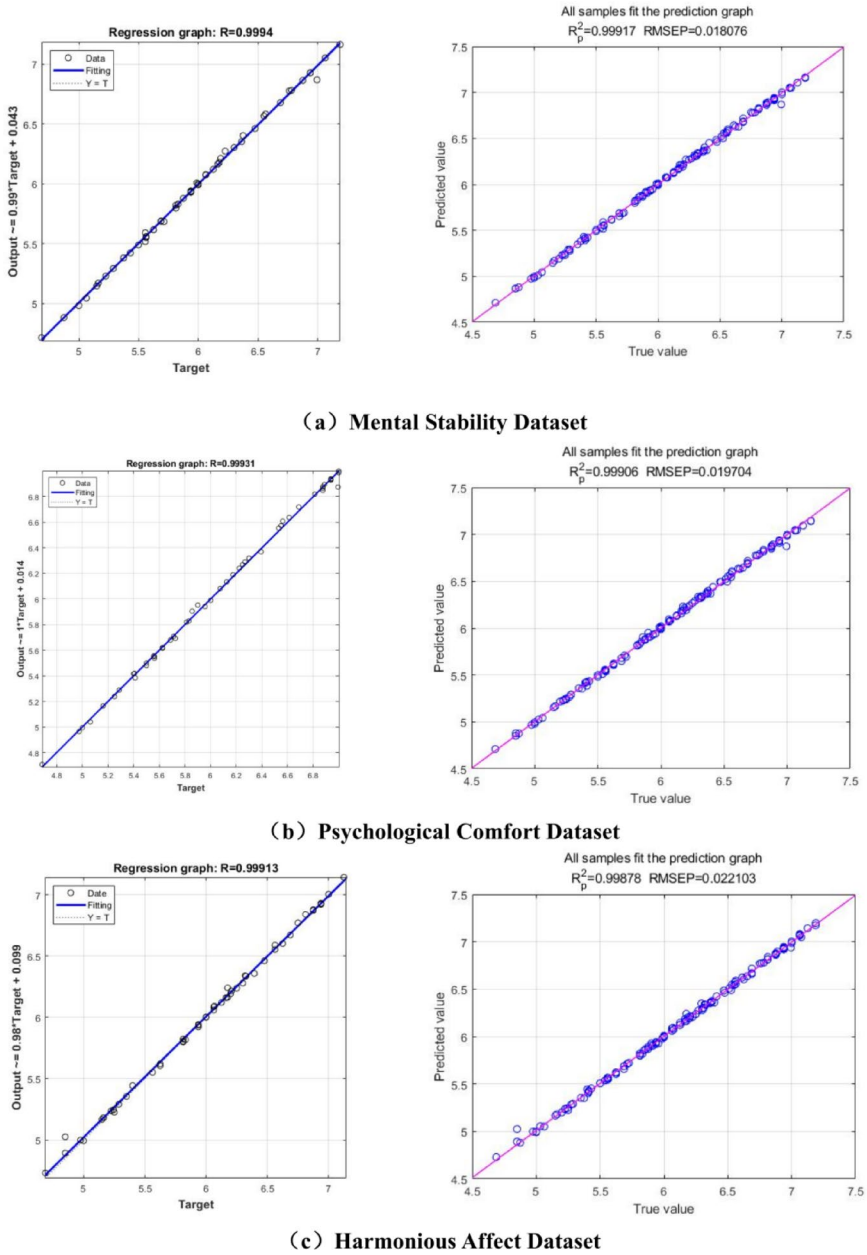

Fig. 20. Model Bus Fitting for User Sentiment Dataset. **a** to **c** Linear fitting plots for the Mental Stability, Psychological Comfort, and Harmonious Affect datasets, respectively.

Experimental results

During the prediction process, the raw data for a given component (e.g., the bracket) were first normalized to mitigate scale differences. The data matrix was then transposed to conform to the input structure of the CPO-CNN-LSSVM model. The model parameter settings utilized the results from the parameter analysis conducted during the preliminary experimental phase.

The features optimized by the CPO algorithm were used as input to the LSSVM for training the model. The experimental results, shown in Fig. 21, demonstrate the relative impact of the four categories of design features on model performance.

The overall linear fitting results, presented in Fig. 22, indicate that the CPO-CNN-LSSVM model achieves an excellent fit between product design features and Miao ethnic style features. The model's coefficient of determination (R^2) consistently exceeded 0.9, approaching 1.0, which indicates that the model explains the vast majority of the observed variance. Similarly, the Root Mean Square Error of Prediction (RMSEP) remained consistently low, further confirming the model's high predictive accuracy. The close clustering of most data points (blue) around the fitted line in Fig. 22 reflects accurate predictions for the majority of samples.

Following training, eight new style feature combinations were input into the model to generate emotional prediction values for 50,000 design variants. The Miao ethnic style combination #3744 achieved the highest

	Cross-stitch	Life meaning	Symmetry	Story-telling	Concrete form	Continuity	Pictographic	Richness	Bracket
1	8	9	7	8	8.8	7.5	8	7	5
2	8.2	8.8	7.2	8.3	8.2	8	7	7.2	4
3	9	9	8	7	8.8	7.5	8.2	8	4
4	9	9.4	9	9	9	7.5	7.9	9	3
5	8	8	9	7	8.8	7	8.5	7	2
6	7	9	8	8	8.2	7	8.2	9	5
7	3	9	9	8	8	7.6	8.4	9	4
…	…	…	…	…	…	…	…		
195	8	8	7	7	7.9	7	7.5	9	5
196	9	8.7	7	7	7.9	7.5	8.5	8.8	3
197	8	8	7.9	7.9	7.8	7.4	8	9	5
198	3	8	9	7	7	7	8	9.4	4
199	8	8	9	7	7	7	8.5	8	4
200	9	8	8	7	7.9	7	8	9	3

Table 15. Matrix for mapping interior features to user emotions.

predicted user emotional rating (9.11), confirming its suitability as the optimal style scheme for preliminary design feature selection. This outcome not only provides a crucial reference for clever fan design but also validates the application value of traditional Miao ethnic style features within modern industrial design.

Design practice

Practice process

In this phase, the previously identified optimal design features and Miao ethnic style elements were integrated into the design implementation. The product modeling was performed using Rhino 9, and rendering was completed using KeyShot 11.

The design implementation focused on a temperature-controlled fan as a prototype for a smart home product. This fan was selected for its alignment with household needs, including compact size, ease of use, durability, and low cost. A color palette of black, blue, and brown was adopted. These hues were chosen to reflect the distinctiveness of Miao culture while ensuring harmony with overall home environments. Morphologically, the design drew inspiration from the iconic form of the Miao long drum, which was skillfully integrated into the fan's main body to highlight the unique charm of Miao culture. For decorative elements, auspicious totem patterns from Miao culture were selected. These motifs were artistically adapted and transformed for integration into the fan's ornamental design, thereby infusing the product with a rich ethnic cultural atmosphere. Prioritizing safety, non-toxicity, low cost, and durability, ABS plastic was selected as the primary material to ensure safe usage.

The design process prioritized the integration of distinctive Miao cultural elements. Iconic symbols, such as the sun god, tree motifs, and floral patterns, were innovatively incorporated into the fan's design. This approach not only enriches the product's cultural depth but also enhances its artistic value, thereby addressing the emotional connection that users have with traditional ethnic patterns. Functionally, the fan incorporates innovative voice recognition technology, which significantly improves operational convenience and user experience. Additionally, the unique pattern design on the fan's outer ring incorporates LED lighting whose intensity automatically adjusts with fan speed, creating a dynamic and engaging living environment.

Design outcomes

Kansei engineering is pivotal in smart home product development, as it focuses on the systematic analysis of users' sensory experiences and emotional responses. This analysis strengthens the emotional connection between users and products, thereby enhancing aesthetic quality, user satisfaction, and ultimately, market competitiveness. The integration of traditional cultural elements with modern innovative products is particularly valuable, as it facilitates cultural preservation while significantly enhancing the visual and sensory experience. Therefore, developing such products requires careful consideration of the appropriate application of cultural elements, fluidity of form lines, and harmonious proportions.

Previous studies have primarily relied on qualitative analyses for evaluating the aesthetic attributes of smart home products, often lacking robust quantitative methodologies. Although design parameter adjustments can significantly impact downstream processes, research systematically exploring product configurations from a green design perspective remains limited. To address this gap, this study introduces an integrated framework combining FAHP, FQFD, and CPO-CNN-LSSVM during the early stages of product development to determine the optimal design combination based on key emotional factors.

Using a smart home fan as a case study, the FAHP method was applied to analyze user emotional needs and perceptions of Miao ethnic style characteristics. Core emotional and stylistic features were quantitatively extracted, leading to the identification of three key perceptual dimensions: "Intelligent Stability," "Emotional Comfort," and "Harmonious Charm." To connect these dimensions with product design features, a morphological analysis was conducted, identifying six categories of design characteristics encompassing 100 specific manifestations. To manage the complexity arising from feature diversity, the FQFD method was employed to select four key

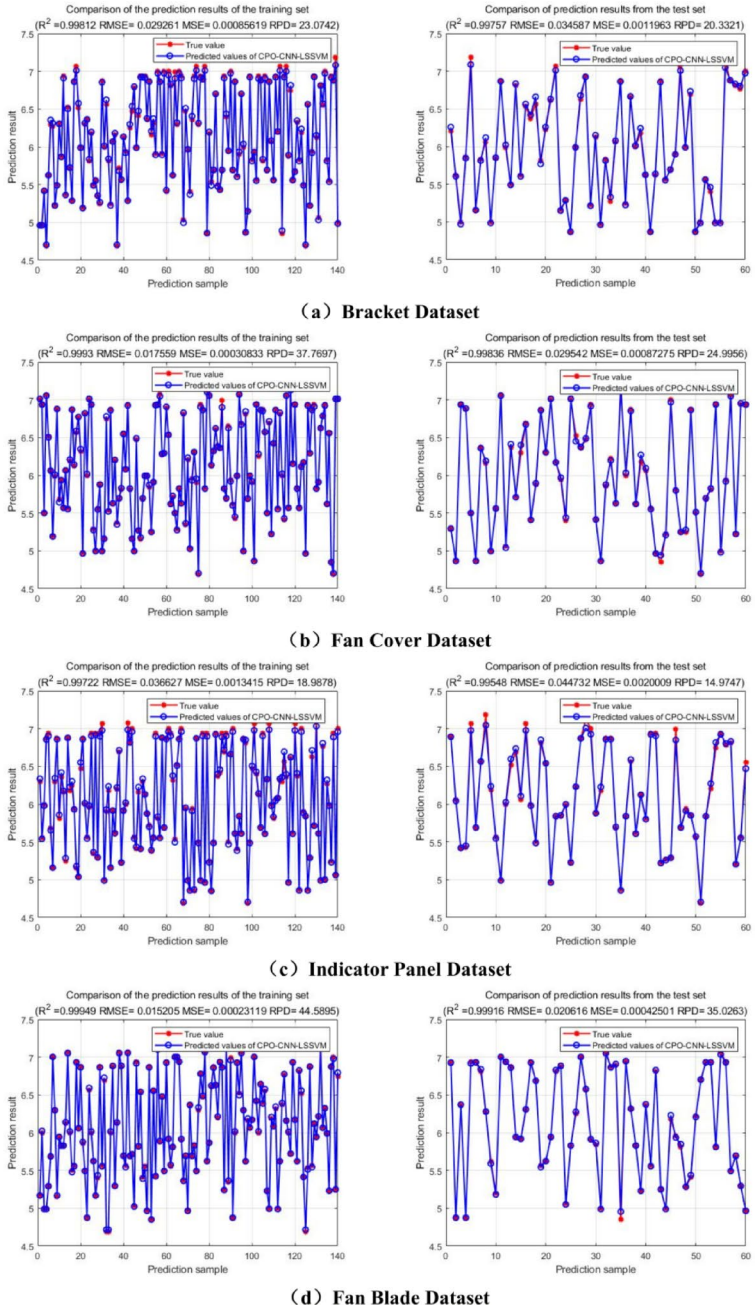

Fig. 21. Performance Evaluation of the CPO-CNN-LSSVM Model on the Designed Feature Dataset. **a** to **d** The performance comparisons between the training and testing sets for the Bracket, Fan Cover, Indicator Panel, and Fan Blade datasets.

functional features (stand, fan cover, indicator panel, and fan blades) and eight key Miao ethnic style features (e.g., cross-stitch, symmetry, and pictographic symbols).

By mapping these datasets within the LSSVM framework, a novel bright fan design concept was developed to predict and recommend optimal design configurations. The analysis demonstrated that a specific configuration (Model 7 for the bracket, Model 5 for the fan cover, and Model 6 for both the indicator panel and fan blades), combined with the eight Miao-style features, effectively satisfies user emotional needs and significantly enhances the sensory experience of the smart fan.

Discussion

Application advantages of the optimized model

Affective engineering provides a comprehensive framework for examining the connection between emotional needs in traditional cultures and modern product aesthetics, thereby bridging the gap between these domains and addressing users' emotional demands for both traditional and contemporary products. Within the affective

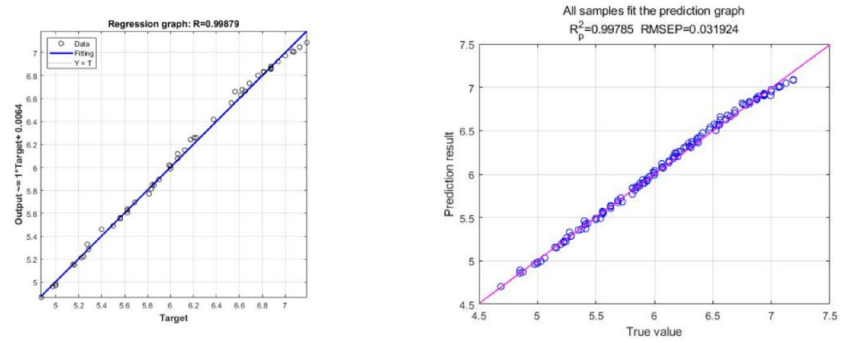

（a）Bracket Dataset

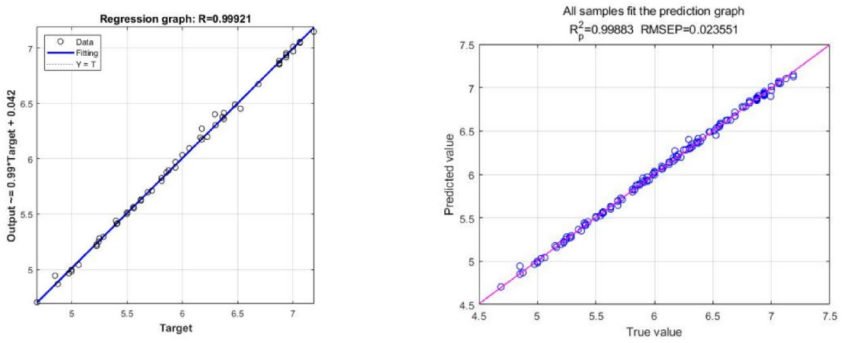

（b）Fan Cover Dataset

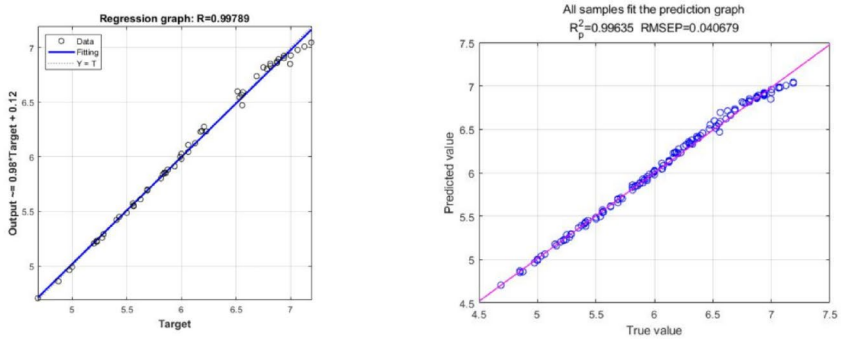

（c）Indicator Panel Dataset

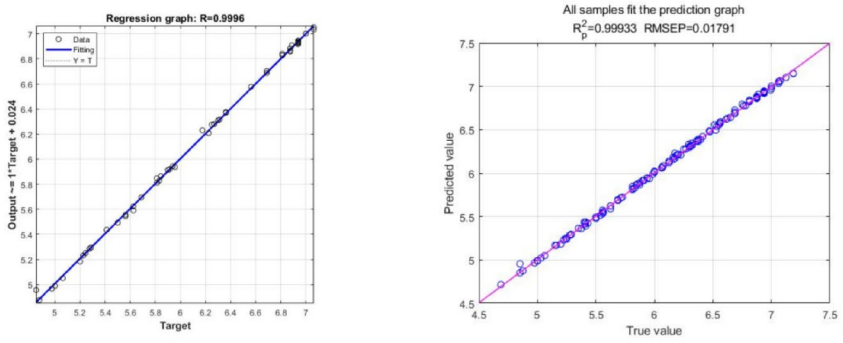

（d）Fan Blade Dataset

Fig. 22. Model bus fitting for design feature dataset. **a** to **d** Lsinear fitting plots for the Bracket, Fan Cover, Indicator Panel, and Fan Blade datasets, respectively.

engineering framework, determining feature weights is crucial for reducing designers' cognitive burden and improving development efficiency. However, traditional feature weighting methods—including the Analytic Hierarchy Process (AHP), KANO model, and subjective evaluation—are often susceptible to evaluators' subjective biases, which can compromise the reliability and scientific rigor of the results. In contrast, the FAHP and FQFD mitigate subjective bias by incorporating fuzzy mathematics theory, thereby improving the accuracy and objectivity of evaluations. Therefore, this study employed FAHP and FQFD to evaluate the emotional

needs and design features of smart home fans, demonstrating superior objectivity and accuracy over traditional methods.

Traditional linear statistical methods, such as Quantification Theory Type II (QT-II) [43] and Principal Component Analysis (PCA) [44], often struggle to capture the inherent subjectivity and nuanced aspects of user emotions when constructing analytical models for design features and emotional factors. Nonlinear statistical methods primarily include artificial intelligence techniques such as neural networks [45], association rule mining (ARM) [46], and genetic algorithms [47]. These methods provide high flexibility and adaptability, enabling a deeper exploration of user emotional information. However, each method has limitations: neural networks require manual parameter configuration; ARM is limited to discrete variables [48]; and genetic algorithms yield a finite set of solutions [49].

Compared to traditional linear methods and neural networks, the Least Squares Support Vector Machine (LSSVM) is particularly well-suited for pattern recognition with small sample sizes, nonlinearity, and high-dimensional data, effectively mitigating the risks of local minima and overfitting. The CPO-CNN-LSSVM model proposed in this study represents an advanced hybrid intelligent framework. It integrates the Crested Porcupine Optimizer (CPO) for automatic optimization, utilizes a Convolutional Neural Network (CNN) for deep feature extraction, and employs LSSVM for efficient classification or regression. Compared to existing methods—including PSO-CNN-SVM, GWO-CNN-LSSVM, GA-CNN-SVM, CNN-LSTM, CNN-GRU, SVM, RF, and XGBoost—the CPO-CNN-LSSVM model demonstrates comprehensive advantages.

Specifically:

Compared to optimization-driven models such as PSO-CNN-SVM and GWO-CNN-LSSVM, the Crested Porcupine Optimizer (CPO) achieves a superior balance between global exploration and local exploitation through its simulation of multiple defense strategies. This approach mitigates the premature convergence of Particle Swarm Optimization (PSO) and enhances the population diversity of the Grey Wolf Optimizer (GWO), resulting in more optimal hyperparameter configurations [50].

(2) Compared to GA-CNN-SVM, which uses genetic algorithm optimization, CPO exhibits faster convergence and greater optimization stability [51].

(3) Compared to deep temporal models such as CNN-LSTM and CNN-GRU, CPO-CNN-LSSVM demonstrates superior generalization and overfitting resistance in small-sample scenarios, along with reduced model complexity and computational overhead [52,53].

(4) Compared to traditional machine learning methods (SVM, RF, XGBoost), CPO-CNN-LSSVM enables end-to-end automatic feature extraction via CNNs, eliminating the need for manual feature engineering and improving feature representation for complex raw data [29,55].

In summary, CPO-CNN-LSSVM achieves comprehensive improvements in parameter search efficiency, feature learning, small-sample adaptability, and classification accuracy through the integrated combination of optimization, feature extraction, and classification components. This framework offers a robust and advanced solution for analyzing high-dimensional nonlinear data (Fig. 23).

Model performance validation

To validate the practical performance and effectiveness of the CPO-CNN-LSSVM model in predicting user sentiment needs, a systematic comparison was conducted against several benchmark machine learning models. A unified dataset served as the benchmark for evaluation, with a focus on key metrics including the coefficient of determination (R^2), root mean square error (RMSE), and mean absolute percentage error (MAPE). To ensure reproducibility and statistical robustness, all models were evaluated using 100 iterations of Bootstrap resampling validation. A comprehensive set of evaluation metrics was examined, including mean absolute error (MAE), RMSE, MAPE, R^2, 95% bias-corrected and accelerated (BCa) confidence intervals, and p-values. The experimental results are summarized in Table 16 and illustrated in Fig. 24.

The analysis indicates that the CPO-CNN-LSSVM model significantly outperforms all benchmark models, including PSO-CNN-SVM, GWO-CNN-LSSVM, CNN-LSTM, SVM, RF, and XGBoost, across all evaluated metrics. Specifically, the CPO-CNN-LSSVM model achieved the lowest values for error metrics (MAE, RMSE, MAPE), while its R^2 value was closest to 1, demonstrating superior predictive accuracy and interpretability. Furthermore, the 95% BCa confidence interval for its R^2 value is the narrowest, indicating higher stability and reliability compared to other models.

In summary, CPO-CNN-LSSVM demonstrates clear advantages across multiple performance metrics and rigorous statistical validation, confirming its suitability for high-dimensional, nonlinear prediction tasks that involve user sentiment analysis.

Exploring design feature interpretability based on SHAP values

Exploring interpretability for user sentiment datasets

To further investigate the relationship between design features and user sentiment, the SHAP (Shapley Additive exPlanations) interpretable machine learning method [52] was employed. This approach quantifies the contribution of each design feature to predicting user sentiment, providing data-driven support and practical guidance for modern product design applications.

A systematic analysis of the results from three chart sets (Figs. 25, 26, 27) reveals distinct influence patterns of design features on user sentiment across three dimensions: feature impact, priority, and dependency. The key findings are as follows:

First, the SHAP value swarm plots in Fig. 25 allow for an intuitive observation of the intensity, direction, and distribution of each feature's influence. Across all three datasets, the fan cover shows the most dispersed point distribution, with SHAP values spanning both positive and negative ranges, indicating that it is the most influential and sensitive feature. This influence is likely driven by factors such as material texture, grille transparency, and

Fig. 23. Product rendering image.

Model	MAE (%)	RMSE(%)	MAPE (%)	R^2	95% BCa CI (R^2)	p-value (vs. CPO)
CPO-CNN-LSSVM	1.23	1.87	3.45	0.982	[0.928, 0.956]	-
PSO-CNN-SVM	1.45	2.12	4.12	0.918	[0.902, 0.934]	0.013
GWO-CNN-LSSVM	1.38	2.05	3.98	0.935	[0.910, 0.940]	0.022
GA-CNN-SVM	1.52	2.20	4.35	0.905	[0.888, 0.922]	0.005
CNN-LSTM	1.67	2.38	4.80	0.890	[0.872, 0.908]	0.001
CNN-GRU	1.62	2.31	4.65	0.895	[0.878, 0.912]	0.002
SVM	2.10	2.85	6.20	0.832	[0.810, 0.854]	< 0.001
RF	1.88	2.60	5.50	0.865	[0.845, 0.885]	< 0.001
XGBoost	1.79	2.48	5.10	0.878	[0.858, 0.898]	< 0.001

Table 16. Model performance validation test.

overall stylistic language. For example, a coarse texture from low-quality plastic, an oppressive sensation from overly dense grilles (negative SHAP values), or safety concerns from sharp edges can significantly diminish perceptions of stability and harmony. Conversely, refined textures, elegant forms, and appropriate transparency enhance the user experience. The bracket also demonstrates a strong bidirectional influence, rooted in the user's innate demand for structural stability. A wobbly or noisy bracket can persistently trigger doubts about product reliability and safety (negative SHAP values). This impact is particularly pronounced in the psychological comfort dataset (Fig. 25b), underscoring that physical security is foundational to comfort. Additionally, in the psychological comfort dataset (Fig. 25b), the point distribution for fan blades is more dispersed than in the other analyses. Blade design directly determines the softness of airflow and noise level—physical sensations that profoundly impact psychological comfort, even surpassing the importance of visual interfaces in this context.

Second, the feature importance rankings in Fig. 26 provide quantitative support for these observations. For both psychological stability and harmonious emotion (Fig. 26a and c), the ranking is consistent: Fan Cover (0.75) > Bracket (0.65) > Indicator Panel (0.45) > Fan Blades (0.35). This suggests that static visual design and structural integrity are crucial in establishing long-term, positive psychological experiences. However,

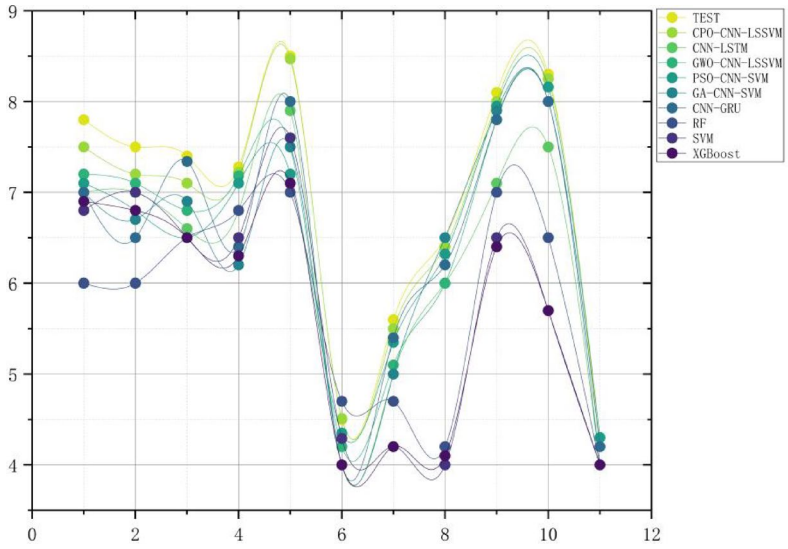

Fig. 24. Algorithm fitting test.

for psychological comfort (Fig. 26b), the ranking shifts to: Fan Cover (0.85) > Bracket (0.78) > Fan Blades (0.68) > Indicator Panel (0.42). This shift significantly elevates the importance of fan blades. When the focus shifts from aesthetics ("how it looks") to performance ("how it performs"), parameters tied to physical sensation (e.g., airflow, noise) take precedence over static interface design. This implies that achieving exceptional comfort requires elevating the aerodynamic and acoustic performance of the blades to a strategic priority on par with visual design.

Finally, the feature dependency analysis in Fig. 27 reveals nonlinear relationships between specific design parameters and user experience. The grille density of the fan cover exhibits a pronounced inverted U-shaped relationship, with its positive contribution to perceived stability peaking within the 0.4–0.6 range (SHAP value ≈ 1.2). Both low (< 0.2) and high (> 0.8) densities yield adverse effects. The bracket's stability parameter shows an asymptotic pattern: beyond a value of 0.7, its marginal contribution to comfort decreases significantly. This finding provides an economical boundary for structural design, indicating a point of diminishing returns. The rotational speed of the fan blades exhibits a two-stage characteristic: a linear increase in contribution to comfort at low speeds (0–0.4), followed by a plateau or decline at high speeds (> 0.6) due to noise interference.

In summary, the three figures form a complete analytical chain: Fig. 25 reveals influence patterns, Fig. 26 determines their priority, and Fig. 27 identifies specific optimization directions. This analysis provides clear guidance for experience-driven design: (1) prioritize fan cover aesthetics and safety, and bracket stability, to build trust; (2) focus on fan blade performance for optimal comfort; and (3) ensure the indicator panel provides seamless auxiliary interaction. Future work could leverage the dependencies shown in Fig. 22 to perform precise parameter optimization for each feature.

Exploring interpretability of product design feature datasets

To further investigate the relationship between design features and traditional cultural elements, SHAP values were again employed to quantify the contribution of each Miao ethnic element to the prediction of user sentiment, providing actionable insights for their application. The impact of Miao-style features on user perception across various innovative fan components was systematically analyzed using SHAP, an explainable machine learning method. Based on three sets of graphical results (Figs. 28, 29, 30), the application effectiveness of traditional cultural elements is examined across three dimensions: feature influence, priority, and dependency.

First, the SHAP summary plot (Fig. 28) reveals that the influence of Miao-style features is distinctly component-specific. Within the bracket component, Figurative Form and Symmetry show the widest distribution of SHAP values, indicating user sensitivity to structural integrity and visual balance. This finding is consistent with engineering psychology principles, suggesting that users perceive the bracket as a visual indicator of product safety. In fan cover design, Continuity and Symmetry are the most influential features, validating the aesthetic value of Miao pattern principles (e.g., spiral motifs, geometric repetition) in contemporary products. Notably, for the control panel, while Continuity is important, symbolic features (such as narrativity and the meaning of Life) have a weaker influence, likely reflecting a user's priority for functional clarity in interactive interfaces.

Second, the feature importance rankings in Fig. 29 quantify the relative importance of features, further revealing design priorities. The analysis indicates that Symmetry and Continuity maintain high importance across components, suggesting they represent universal core values of Miao style in contemporary design. In the fan blade component, the importance of Symmetry (0.55 +) significantly exceeds that of other features, likely because dynamic rotation amplifies its visual impact. In contrast, narrative features (e.g., Narrativity, Meaning of Life) show relatively low importance across all components. This finding suggests that modernizing ethnic styles should prioritize the transformation of visual forms over the direct transplantation of symbolic meanings.

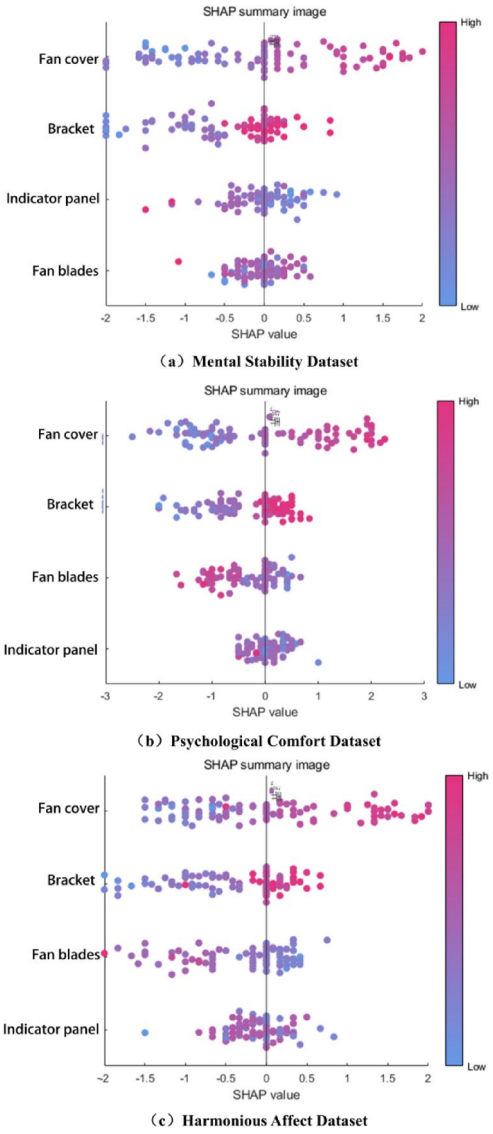

Fig. 25. SHAP value swarm plots for three datasets (Generated by Matlab2024b software). **a** to **c** respectively show the eigenvalue swarm plots for the Mental Stability, Psychological Comfort, and Harmonious Affect datasets.

Finally, the feature dependency diagrams in Fig. 30 provide deeper insight by revealing complex nonlinear relationships between feature values and their contributions (SHAP values). For the bracket component (Fig. 30a), Figurative Form shows a distinct inverted U-shaped relationship. When the morphological integrity parameter is between 0.4 and 0.6, its contribution reaches its peak, with SHAP values of 0.35. This indicates an optimal range for morphological integrity, beyond which user experience diminishes. The Continuity feature for the fan cover (Fig. 30b) exhibits a sigmoidal (S-shaped) dependency curve. When the continuity value is below 0.3, the SHAP value increases slowly (< 0.1); between 0.3 and 0.7, it rises sharply to over 0.4; and beyond 0.7, the growth plateaus. This pattern provides quantitative guidance, suggesting an optimal range of continuity parameters of 0.5 to 0.7. For the fan blade component (Fig. 30d), the Symmetry feature exhibits a distinct dynamic effect. At low speeds (parameter < 0.4), SHAP values are low (Approximately 0.2); at medium to high speeds (0.4–0.8), they increase linearly to 0.55; and at very high speeds (> 0.8), they decrease by approximately 10%, likely due to visual persistence effects. This suggests that blade design must account for dynamic visual effects during operation. For the indicator panel (Fig. 30c), narrative features (e.g., Narrativity) exhibit flatter dependency curves with more minor fluctuations in SHAP values (0.1–0.25). This indicates a limited scope for parameter adjustment and underscores the need for caution when incorporating such elements into functional interfaces.

From a design perspective, the analysis yields key insights: Miao ethnic style requires differentiated application strategies across components. Structural components (e.g., brackets) should emphasize Figurative Form and Symmetry; aesthetic components (e.g., fan covers) can highlight Continuity and decorative details; and interactive components (e.g., indicator panels) should simplify cultural symbols. Continuity and Symmetry show high modern adaptability, whereas narrative-based symbols require innovative expression integrated

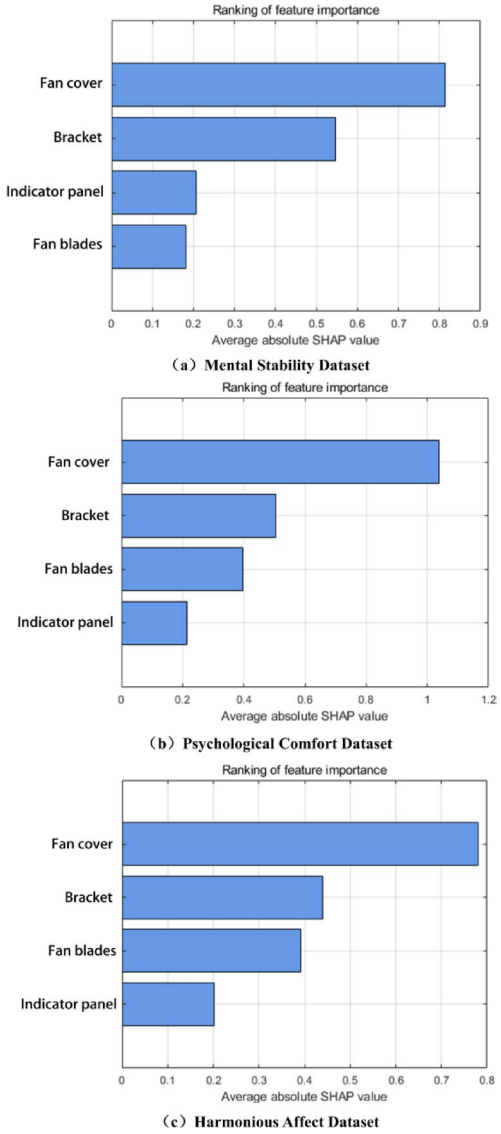

Fig. 26. Feature importance ranking for three datasets (Generated by Matlab2024b software). **a** to **c** respectively show the feature importance rankings for the Mental Stability, Psychological Comfort, and Harmonious Affect datasets.

with contemporary aesthetics. For moving components (e.g., blades), dynamic viewing conditions must be considered, emphasizing Continuity over intricate details.

A limitation of this study is the insufficient consideration of perceptual differences among users from diverse cultural backgrounds. Future research should investigate the optimal combinations of traditional and modern features, as well as the moderating role of cultural identity in product preference. Deepening the understanding of the principles for translating traditional cultural elements into modern design will advance the creative transformation and innovative development of national culture.

Application potential and limitations of the model

The CPO-CNN-LSSVM hybrid model employed in this study demonstrates strong performance in mapping intelligent fan design features to user emotional responses. This is achieved by optimizing the integration of Convolutional Neural Networks (CNN) and Least Squares Support Vector Machines (LSSVM) through the Crown Porcupine Optimization (CPO) algorithm. Based on the model's characteristics and practical application, we explore its broader application potential and core limitations as follows.

The CPO-CNN-LSSVM model possesses unique advantages in handling complex mappings between product design features and user emotional responses, with potential applications extending to multiple related fields. In medical device design, this model holds significant value. Taking home medical devices (e.g., blood glucose monitors, blood pressure monitors) as an example, analyzing how features like device form, color, and interface design influence patient psychological comfort can alleviate anxiety associated with medical equipment. Research indicates that gentle form design and soothing color schemes significantly enhance patient treatment compliance,

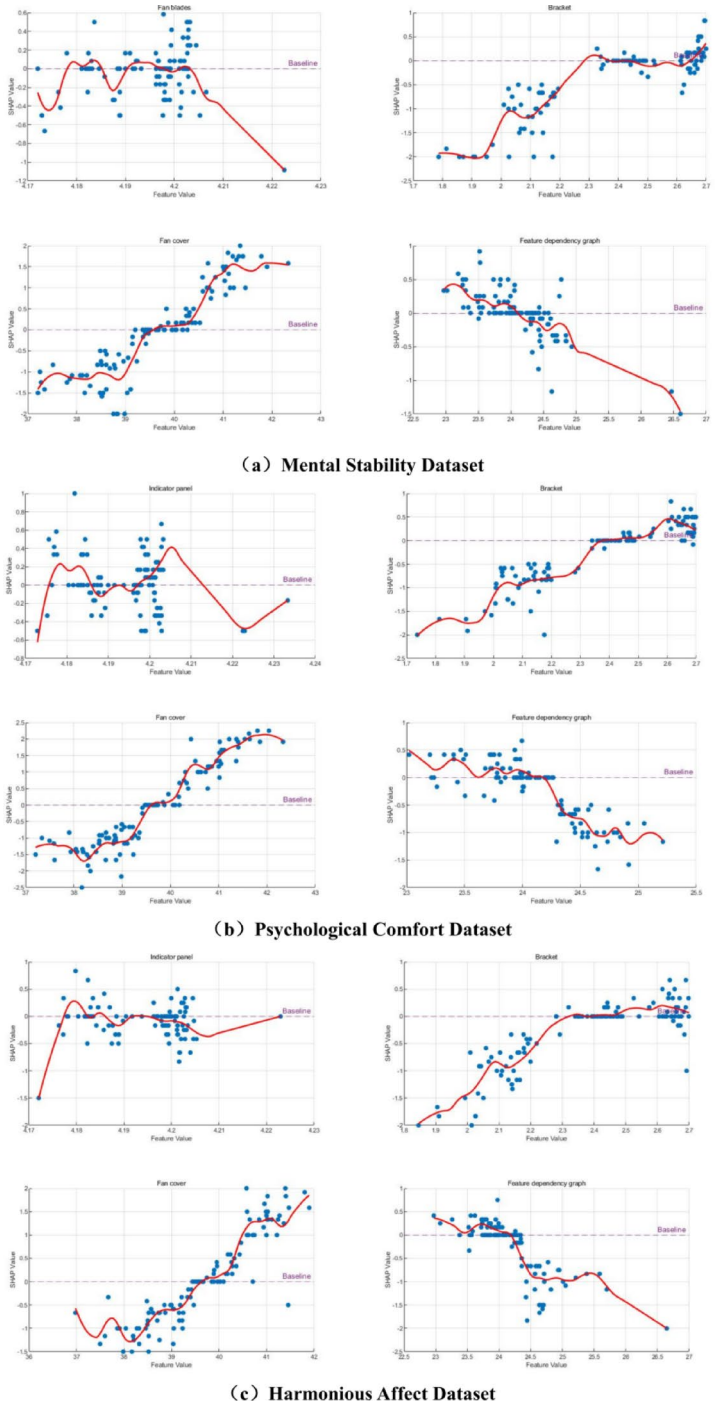

Fig. 27. Feature dependency of three datasets (Generated by Matlab2024b software). **a** to **c** The eigenvalue dependencies for the Mental Stability, Psychological Comfort, and Harmonious Affect datasets.

and this model can provide quantitative support for such design decisions. In the office equipment domain, the model can be applied to optimize workstation design. Analyzing the relationship between design features of office equipment (such as monitors, keyboards, and office chairs) and work efficiency/comfort helps enterprises create work environments that better align with ergonomic and psychological needs. Particularly against the backdrop of increasingly widespread remote work, this model can offer scientific guidance for designing home office equipment. It also holds promising applications in the interior design of vehicles. Interior design for vehicles, such as automobiles and high-speed trains, must strike a balance between aesthetics, functionality, and comfort. By analyzing how various design parameters influence passenger psychological perceptions, this model can provide optimization recommendations for interior design.

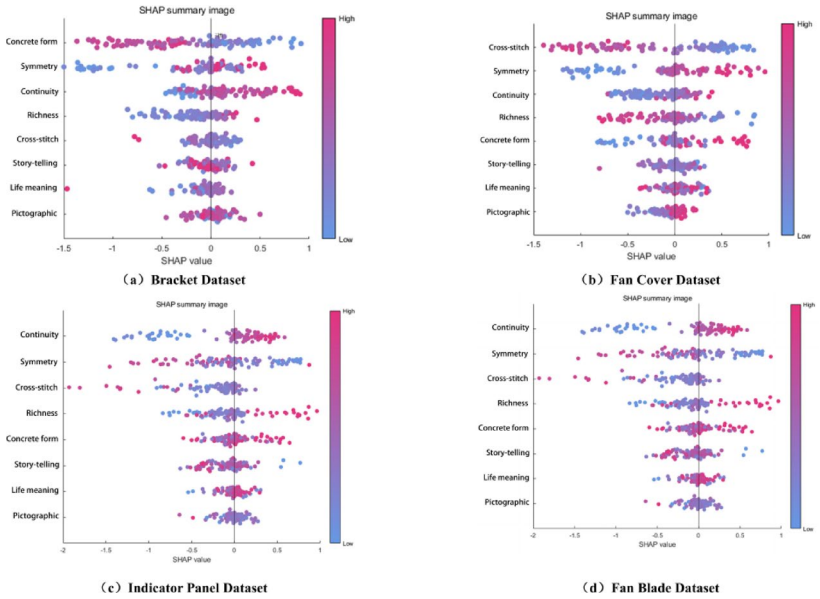

Fig. 28. SHAP value swarm plots for three datasets (Generated by Matlab2024b software) **a** to **d** Swarm values for the Bracket, Fan Cover, Indicator Panel, and Fan Blade datasets, respectively.

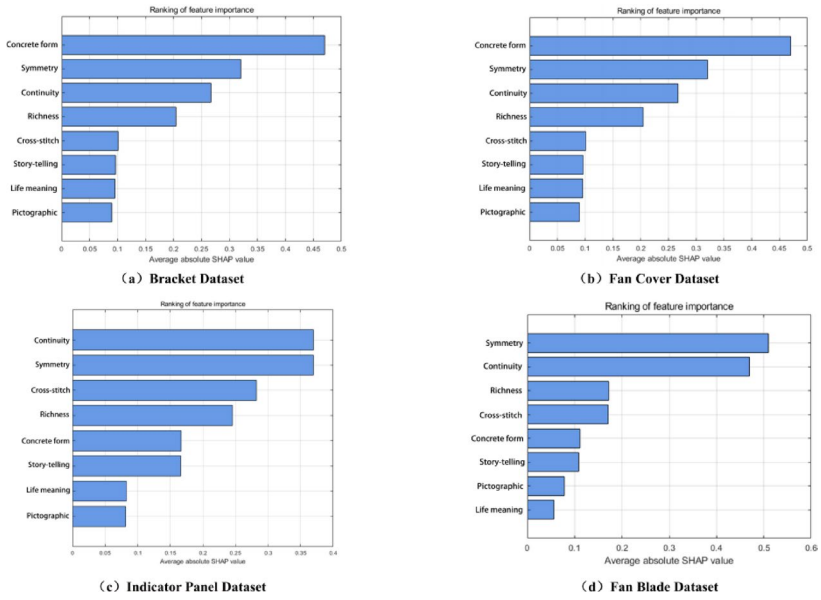

Fig. 29. Feature importance ranking for three datasets (Generated by Matlab2024b software). **a** to **d** The feature importance for the Bracket, Fan Cover, Indicator Panel, and Fan Blade datasets, respectively.

Despite demonstrating application potential across multiple domains, the CPO-CNN-LSSVM model still has core limitations that require addressing:

First, the model exhibits limited domain adaptability. While performing well in the smart fan design context of this study, it requires retraining and parameter adjustments when transferred to other product domains. Significant variations in product design characteristics and user priorities across different fields necessitate strong domain adaptation capabilities, an area where the current model architecture remains deficient.

Second, the model lacks sufficient sensitivity to cultural differences. In a globalized market environment, product design must fully account for perceptual variations among users from diverse cultural backgrounds. Current models are primarily trained on data from a single cultural context, which can introduce biases when addressing cross-cultural design challenges. For instance, certain design elements may evoke positive emotions in one culture while triggering negative associations in another.

Additionally, the model's real-time performance requires improvement. Although the Guanhauzhu optimization algorithm demonstrates strong global search capabilities, its high computational complexity

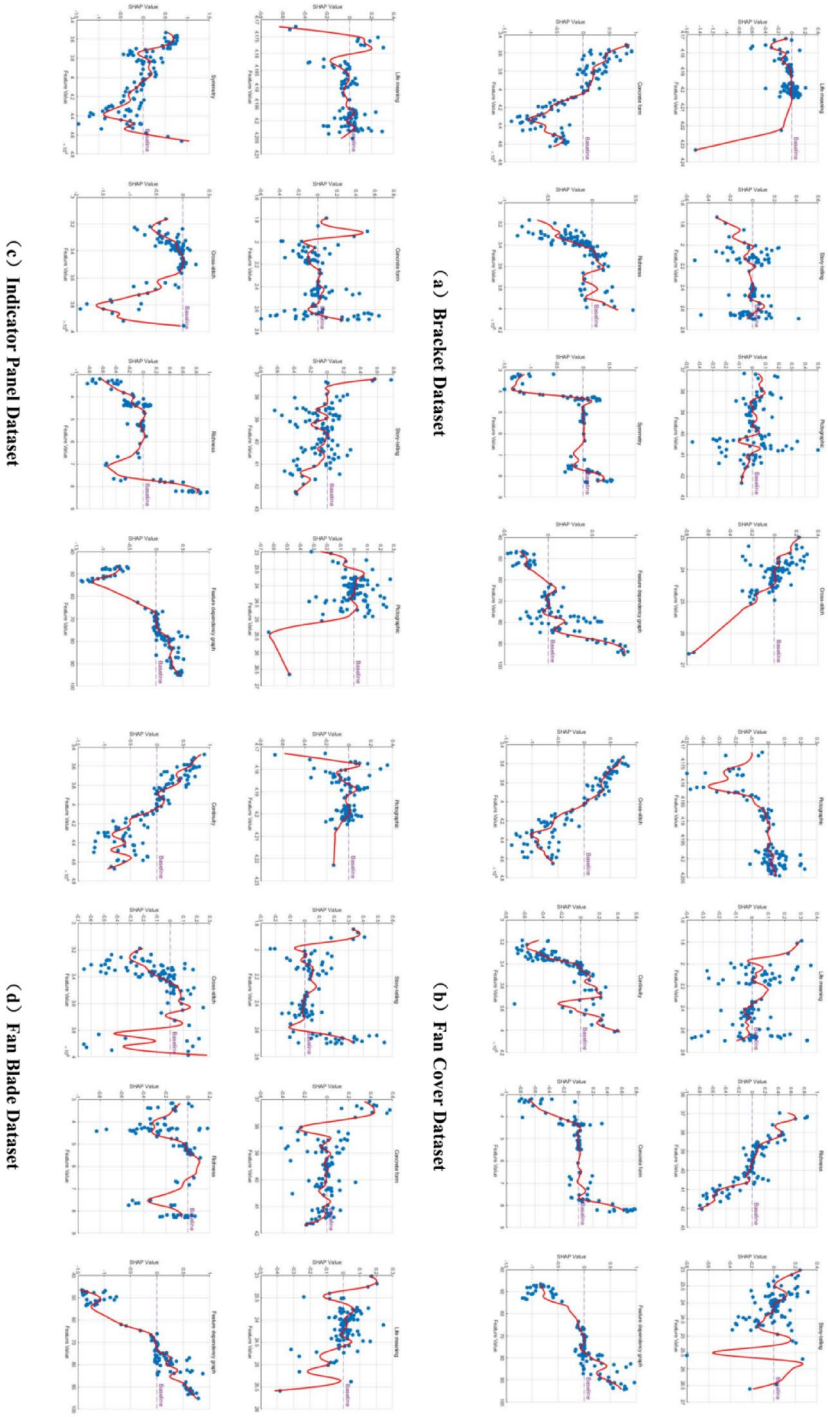

Fig. 30. Feature dependency of three datasets (Generated by Matlab2024b software). **a** to **d** The eigenvalue dependencies for the Bracket, Fan Cover, Indicator Panel, and Fan Blade datasets, respectively.

necessitates extended processing times for large-scale design parameter optimization. This limits the model's applicability in rapid, iterative design processes, particularly in scenarios that require real-time feedback.

At the same time, the sample size used for training the model is relatively limited. Although we have ensured the model's effectiveness for the current task through the aforementioned methods, a larger, cross-category sample repository would undoubtedly further enhance the model's universality and robustness.

Finally, the model exhibits limited adaptability to emerging design trends. Product design aesthetics and user preferences evolve, whereas training data often reflects historical preferences. This may hinder the model's ability to accurately predict user responses to innovative or cutting-edge design styles, necessitating mechanisms for continuous learning and updates.

Conclusions

Traditional machine learning methods are often limited in their ability to capture nuanced user emotional characteristics and cultural semantic contexts, making it difficult to discern genuine emotional needs and cultural connotations accurately. Furthermore, these methods are susceptible to subjective biases during the quantification of user requirements. To address these challenges, this study proposes an innovative framework that integrates fuzzy computing with an enhanced CPO-CNN-LSSVM algorithm. This framework establishes a predictive model capable of addressing both user emotional demands and specific cultural semantic contexts.

First, core Miao ethnic style features and smart home fan design characteristics were quantified using an integrated FAHP and FQFD methodology. These quantified features were then used as variables and combined with expert evaluations to construct the training and validation datasets. The CPO-CNN-LSSVM algorithm was then applied to these datasets to predict optimal combinations of design and cultural features, resulting in a preferred design scheme that served as the basis for practical implementation. The model's performance was validated, confirming its superiority over benchmark methods. Furthermore, SHAP explainability analysis was employed to explore the influence mechanisms of design and cultural features on user emotions, thereby revealing key optimization pathways. This approach facilitates the iterative development of products that align with cultural contexts and user sentiments, while balancing diverse requirements.

This research provides significant insights for the integration of cultural elements into innovative product design, which can be summarized as follows:

1. A Multidimensional Design Feature Quantification System. The integration of FAHP and FQFD provides a robust method for translating ambiguous user needs into concrete design parameters, offering quantifiable support for decision-making.
2. Innovations in Algorithmic Architecture. The proposed CPO-CNN-LSSVM framework demonstrates distinct advantages. The Crested Porcupine Optimizer (CPO) mitigates the local optimum convergence typically found in traditional methods, efficiently locating global optima. The CNN module excels at automatic feature extraction, while the LSSVM maintains strong generalization capabilities with small sample sizes.
3. A Balance of Interpretability and Practicality. The incorporation of SHAP provides not only predictions but also insights into the mechanisms linking design to emotion, transforming the process from a "black box" to a transparent one and enhancing practical utility.

Despite these contributions, the study has limitations that indicate areas for future improvement:

1. Limited Sample Scope. The findings are based primarily on data from specific user groups. Future work should include more diverse cohorts (e.g., individuals of different ages and cultural backgrounds) to enhance the generalizability of the results.
2. Computational Intensity. The computational complexity of CPO limits its use in real-time applications. Future research should investigate more efficient optimization algorithms or model compression techniques to improve practicality.
3. Limited Cross-Cultural Adaptability. The model's sensitivity to cultural differences is insufficient. Future studies should incorporate multicultural perspectives and establish cross-cultural evaluation frameworks to enhance global market applicability.
4. Dataset Diversity. We are committed to expanding the scale and diversity of our datasets by collecting data on a wider range of smart home products and cultural elements to train more universally applicable cultural affective design prediction models.

Future research directions include: (1) developing dynamic update mechanisms for the model to adapt to evolving trends and preferences; (2) creating practical design assistance tools based on the findings; and (3) investigating multimodal data fusion, incorporating physiological signals, to improve emotion recognition accuracy.

Data availability

Data is provided within the manuscript.

Received: 8 October 2025; Accepted: 25 November 2025
Published online: 17 December 2025

References

1. Dai, Q., Liu, J., Wu, Y. & Xu, W. Discussing the protection of Guangxi's intangible cultural heritage from a regional perspective. *Resour. Sci* **35**, 1104–1112 (2013).
2. Ding, C. B., Zhuo, X. L. & Xiao, D. W. Ethnic differentiation in the internal spatial configuration of vernacular dwellings in the multi-ethnic region in Xiangxi, China from the perspective of cultural diffusion. *Heritage Sci.* **12**(1), 3 (2024).
3. Ning, B.Y., Omar, R., Ye, Y. Intergenerational transmission or cultural loss? The continuity of ethnic identity among the Yao minority in China. *Qualit. Res. J.* 2025.
4. Jiang, N. Smart home product layout design method based on real-number coding genetic algorithm. *Comput. Intell. Neurosci*. 2022.
5. Tang, R.Y., Inoue, Y. Services on Platform Ecosystems in the Smart Home 2.0 Era: Elements influencing consumers' value perception for smart home products. *Sensors*. **21**(21);2021.
6. Huang, Y. R., Li, X. X., Ling, S. & Zheng, C. An analysis of how smart home product attributes influence older adults' avoidance psychology: the sequential mediation role of product identity and trust. *Behav. Sci.* **14**, 11 (2024).
7. Tippe, M; Wigger, H; Brand-Daniels, U; Vogt, T. Operationalising user behaviour: a study on the life cycle assessment of smart home technologies. *Energy Sustain. Soc*. **15**(1);2025.

8. Tang, R. Y., Inoue, Y. & Tsujimoto, M. Synergy effect in platform ecosystem: a quantitative analysis of smart home products. *IEEE ACCESS.* **13**, 13482–13506 (2025).
9. Han, S., Shi, Z. & Shi, Y. Cultural and creative product design and image recognition based on the convolutional neural network model. *Comput. Intelligence Neurosci.* **2022**, 2586042 (2022).
10. Cheng, H., Liu, B. J., Sun, X. & Qiu, X. Data-efficient creativity evaluation in museum cultural creative products: a machine learning framework for data-driven decision-making in product development. *Expert Syst. Appl.* **297**, 129014 (2025).
11. Liu, W. J. & Luo, S. W. Redesign of the ming-style `warped table' based on Kansei needs of contemporary users using an SD FA QFD method. *BioResources* **20**(4), 10082–10105 (2025).
12. Hu, D. L., Wang, E. S. & Arshad, M. Design of personalized creation model for cultural and creative products based on evolutionary adaptive network. *PeerJ Comput. Sci.* **11**, e3288 (2025).
13. Wang, T., Hamat, B., Zhang, L. M., Zhao, Y. X. & Pang, L. L. L. Study on the application and evaluation method of Zen aesthetic style in furniture design under the background of sustainability. *Sci. Rep.* **15**(1), 9236 (2025).
14. Xu, T; Song, ZP; Fan, SY; Guo, DS. Improved risk assessment model using the cloud theory of the existing tunnel in foundation pit construction environment. *Eng Construct Architect Manage.* 2025.
15. Li, Z., Tian, Z. G., Wang, J. W. & Wang, W. M. Extraction of affective responses from customer reviews: an opinion mining and machine learning approach. *Int. J. Comput. Integr. Manuf.* **33**(7), 670–685 (2020).
16. Yuan, B. K., Ye, J. N., Wu, X. Y. & Yang, C. X. Applying latent dirichlet allocation and support vector regression to the aesthetic design of medical nursing beds. *J Comput. Inf. Sci. Eng.* **23**(5), 051014 (2023).
17. Wang, N. Y., Shi, D., Li, Z. R., Chen, P. T. & Ren, X. P. Investigating emotional design of the intelligent cockpit based on visual sequence data and improved LSTM. *Adv. Eng. Inf.* **61**, 102557 (2024).
18. Meng, Y. F. et al. Enhancing educational equity and sustainability: a fuzzy-based framework for optimal school site selection. *Int. J. Digit. Earth.* **18**(1), 2495735 (2025).
19. Liu, Z. M., Liang, X. N., Li, L. W., Li, X. Y. & Ou, W. W. Research on sustainable design of smart charging pile based on machine learning. *Symm.-Basel.* **16**(12), 1582 (2024).
20. Wang, T., Chen, H. Z., Hamat, B. & Zhao, Y. X. Research on cultural and creative design method of 2022 World Cup lamps based on AHP-FCE. *PLoS ONE* **19**(12), e0316861 (2025).
21. Wang, T., Zhao, Y. X., Zhang, X. D., Xie, Y. B. & Pang, L. L. L. Design of walking aids for the elderly based on the Kano-AHP-FEC method. *Sci. Rep.* **15**(1), 2663 (2025).
22. SeyedShenava, S; Zare, P; Mohammadian, A. Sustainable transient frequency management in eco-industrial park microgrids considering e-shared mobility storage using efficient fractional-order computing. *Sustain. Comput.-Inform. Syst*. **48**;2025
23. Li, M; Wang, X. Short-term electricity price forecasting via CPO-enhanced dual decomposition and NRBO-optimized deep learning. *Digit. Signal Process*. **168**(B);2025.
24. Zhu, H. X. et al. Lightweight real-time sensor signal reconstruction in nuclear reactors via knowledge distillation and MBSNet. *Ann. Nucl. Energy.* **223**, 111678 (2025).
25. Zhao, Z. Y. et al. IGA-Net: an iterative low-light micro-hole inner wall image enhancement network via global illumination modulation and adaptive feature optimization. *Exp. Syst. Appl.* **297**, 129492 (2025).
26. Zhao, Y. R. et al. Improving the prediction performance of soluble solid content in bagged "Cuiguan" pear using Vis/NIR spectroscopy with spectral correction. *Food Control* **179**, 111596 (2025).
27. Qiu, Y. Q. et al. Minimum cell voltage clamping control of proton exchange membrane fuel cells based on intelligent methods. *Renewable Energy* **256**, 123953 (2025).
28. Zhao, C., Ye, J. C., He, P., Zhang, S. H. & Fan, J. L. Two-stage data-driven adaptive robust bidding model for a virtual power plant in multi-market based on nonparametric method of LSSVM-AKDE under uncertainties. *Renewable Energy* **256**, 123768 (2025).
29. Budhathoki, M. et al. Market dynamics and E-commerce satisfaction in China's aquatic food sector: Machine learning and data insights. *Aquaculture* **610**, 742904 (2025).
30. Sun, Z. L., Zhang, Y. Y., Hong, Z. J. & Du, J. J. Dual-channel surface-enhanced Raman spectroscopy integrated with machine learning for accurate classification of mixed dyes. *Spectrochimica Acta Mole Biomole. Spectroscopy.* **346**, 126859 (2025).
31. Ostmann, P., Kremer, M. & Mueller, D. Identifying and optimizing the aeroacoustic source regions of a slot air diffuser. *Appl. Acoust.* **241**, 111002 (2025).
32. Bonello, A., Brown, C. A., Francalanza, E., Gauci, M. V. & Refalo, P. A novel human-centred approach using Axiomatic Design and Kansei engineering for designing physically and cognitively safe human-robot collaborative workstations. *Product. Manufact. Res. Open Access J.* **13**(1), 2508451 (2025).
33. Liu, J., Gao, H. H. & Yezhova, O. Generative design of bamboo furniture combining game theory and AI-generated content. *BioResources* **20**(4), 8611–8631 (2025).
34. Li, XL; Zhang, YH; Zhang, RR; Yin, YL; Yuan, QY; Li, HM. Evolution path, hot spots and frontiers of big data research in the construction industry from 2010 to 2024. *Eng. Construct. Archit. Manage*. 2025.
35. Yang, D., Liu, L., Bai, W. C. & Tian, W. Y. Conceptual design and configurations selection of S/H-UAVs based on Q-rung dual hesitant double layer FQFD. *Chin. J. Aeronaut.* **37**(9), 193–205 (2024).
36. Liu, Z. M., Chen, X. H. & Liang, X. A. Growable design of passenger vehicle interior space based on FAHP and FQFD. *PLoS ONE* **19**(6), e0303233 (2024).
37. Ren, J., Tian, D. L., Zheng, H. X., Wang, G. S. & Li, Z. K. Research on interval probability prediction and optimization of vegetation productivity in hetao irrigation district based on improved TCLA model. *Agron.-Basel.* **15**(6), 1279 (2025).
38. Uluocak, I. & Bilgili, M. Daily air temperature forecasting using LSTM-CNN and GRU-CNN models. *Acta Geophys.* **72**(3), 2107–2126 (2023).
39. Chen, L. & Zhou, S. S. Sparse algorithm for robust LSSVM in primal space. *Neurocomputing* **275**, 2880–2891 (2018).
40. Abdel-Basset, M., Mohamed, R. & Abouhawwash, M. Crested Porcupine Optimizer: A new nature-inspired metaheuristic. *Knowl-Based Syst.* **284L**, 111257 (2024).
41. Wang, M. Z. et al. Modified MF-DFA Model Based on LSSVM Fitting. *Fractal Fract.* **8**(6), 320 (2024).
42. Mustaffa, Z. & Yusof, Y. LSSVM parameters tuning with enhanced artificial bee colony. *Int. Arab J. Inform. Technol.* **11**(3), 236–242 (2014).
43. Zamenina, E. V., Panteleeva, N. I. & Roshchevskaya, I. M. The electrical activity of the human heart during ventricular repolarization under acute normobaric hypoxia before and after interval hypoxic training. *Vestnik Tomskogo Gosudarstvennogo Universiteta-Biologiya.* **48**, 115–134 (2019).
44. Li, H. J. et al. Revolutionizing agricultural stock volatility forecasting: a comparative study of machine learning and HAR-RV models. *J. Appl. Econ.* **28**(1), 2454081 (2025).
45. Barimani, M. & Aghagolzadeh, A. Unsupervised CNN-based pan-sharpening with generative multiadversarial networks: a colorization approach for panchromatic images. *Int. J. Image Data Fusion.* **16**(1), 1–26 (2025).
46. Gutiérrez-Rodríguez, R., Rojí, E. & Cuadrado, J. Identifying relevant patterns between injury crashes and road safety inspection deficiencies. *J. Safety Res.* **93**, 99–134 (2025).
47. Tat, P. V. & Nhung, N. T. A. Insight prediction of receptor binding activity of a set of benzamide derivatives using hybrid QSAR models: GA-MLR and GA-SVR. *Vietnam J. Chem.* **58**(2), 191–200 (2020).
48. Nam, S. H. et al. Design of hybrid lower control arm using finite element analysis. *Trans. Korean Soc. Mech. Eng. A* **44**(1), 49–56 (2020).

49. Chen, Y. P., Dan, Z. W. & Li, S. Q. Measuring endogenous GA and IAA. *Bio-Protoc.* **12**, 4 (2022).
50. Zhou, K. et al. Research on solving flexible job shop scheduling problem based on improved GWO Algorithm SS-GWO. *Neural Process. Lett.* **56**(1), 144 (2024).
51. Guan, S. Y., Wang, X. K., Hua, L. & Li, L. Quantitative ultrasonic testing for near-surface defects of large ring forgings using feature extraction and GA-SVM. *Appl. Acoust.* **173**, 107714 (2021).
52. Zhang, JX; Li, SY. Air quality index forecast in Beijing based on CNN-LSTM multi-model. *Chemosphere*. **308**(1);2022
53. Yunxue, T; Shuo, S; Haonian, Z; Shibiao, X; Yuming, Y; Ming, Z; Shihua, Z. Identification of intensive oscillation parameters of power system based on CS-CNN-GRU network. *Electric Power Components Syst*. 2024.
54. Li, H. W., Hasi, W., Li, N., Liu, X. & Fang, G. Q. Machine learning-enhanced SERS detection of melamine and its analogues in non-pretreated milk via filter-pressing assembled polytetrafluoroethylene-AgNPs substrate. *Spectrochimica Acta Part A-Mole. Biomole. Spectroscopy.* **344**(2), 126751 (2025).
55. Tang, W. W., Dang, C. & Xu, J. Parallel active learning XGBoost for structural reliability analysis with application to an onshore wind turbine tower. *Reliab. Eng. Syst. Safety.* **265**, 111390 (2025).
56. Jiang, J. X. et al. A deep learning framework integrating Transformer and LSTM architectures for pipeline corrosion rate forecasting. *Comput. Chem. Eng.* **204**, 109365 (2025).

Author contributions
Cheng Kai was responsible for verifying this article, overseeing its overall direction, drafting the original text, and processing the data.

Funding
This research received no external funding.

Declarations

Ethical approval
This study was reviewed and approved by the Ethics Committee of Shaanxi University of Science and Technology for conducting the user questionnaire survey. Review Number: IRBSUT20251089. All participants in the experiment participated in this questionnaire survey with full knowledge and consent.

Additional information

Correspondence and requests for materials should be addressed to K.C. or N.V.S.